

Electron EDM arising from modulus τ in the supersymmetric modular invariant flavor models

Morimitsu Tanimoto ^{a,*} and Kei Yamamoto ^{b,c,†}

^a*Department of Physics, Niigata University, Niigata 950-2181, Japan*

^b*Physics Program, Graduate School of Advanced Science and Engineering, Hiroshima University,
Higashi-Hiroshima 739-8526, Japan*

^c*Core of Research for the Energetic Universe, Hiroshima University, Higashi-Hiroshima 739-8526,
Japan*

Abstract

The electric dipole moment (EDM) of electron is studied in the supersymmetric A_4 modular invariant theory of flavors with CP invariance. The CP symmetry of the lepton sector is broken by fixing the modulus τ . Lepton mass matrices are completely consistent with observed lepton masses and mixing angles in our model. In this framework, a fixed τ also causes the CP violation in the soft SUSY breaking terms. The electron EDM arises from the CP non-conserved soft SUSY breaking terms. The experimental upper bound of the electron EDM excludes the SUSY mass scale below 4–6 TeV depending on five cases of the lepton mass matrices. In order to see the effect of CP phase of the modulus τ , we examine the correlation between the electron EDM and the decay rate of the $\mu \rightarrow e\gamma$ decay, which is also predicted by the soft SUSY breaking terms. The correlations are clearly predicted in contrast to models of the conventional flavor symmetry. The branching ratio is approximately proportional to the square of $|d_e/e|$. The SUSY mass scale will be constrained by the future sensitivity of the electron EDM, $|d_e/e| \simeq 10^{-30}$ cm. Indeed, it could probe the SUSY mass range of 10–20 TeV in our model. Thus, the electron EDM provides a severe test of the CP violation via the modulus τ in the supersymmetric modular invariant theory of flavors.

*E-mail address: tanimoto@muse.sc.niigata-u.ac.jp

†E-mail address: keiy@hiroshima-u.ac.jp

1 Introduction

The non-Abelian discrete groups have been discussed to challenge the flavor problem of quarks and leptons in the standard model (SM) [1–10]. Indeed, supersymmetric (SUSY) modular invariant theories give us an attractive framework to address the flavor symmetry of quarks and leptons with non-Abelian discrete groups [11]. In this approach, the quark and lepton mass matrices are written in terms of modular forms which are holomorphic functions of the modulus τ . The arbitrary symmetry breaking sector of the conventional models based on flavor symmetries is replaced by the moduli space, and then Yukawa couplings are given by modular forms.

The well-known finite groups S_3 , A_4 , S_4 , and A_5 are isomorphic to the finite modular groups Γ_N for $N = 2, 3, 4, 5$, respectively [12]. The lepton mass matrices have been given successfully in terms of A_4 modular forms [11]. Modular invariant flavor models have been also proposed on the $\Gamma_2 \simeq S_3$ [13], $\Gamma_4 \simeq S_4$ [14] and $\Gamma_5 \simeq A_5$ [15]. Based on these modular forms, flavor mixing of quarks and leptons have been discussed intensively in these years. Phenomenological studies of the lepton flavors have been done based on A_4 [16–18], S_4 [19–21] and A_5 [22]. A clear prediction of the neutrino mixing angles and the Dirac CP phase was given in the simple lepton mass matrices with the A_4 modular symmetry [17]. The Double Covering groups T' [23, 24] and S'_4 [25, 26] were also realized in the modular symmetry. Furthermore, phenomenological studies have been developed in many works [27–77] while theoretical investigations have been also proceeded [78–97].

The supersymmetric modular invariant theory of flavors addresses not only the flavor structure of quarks and leptons, but also the flavor structure of their superpartners and leads to specific patterns in soft SUSY breaking terms [73, 74]. Soft SUSY breaking terms were studied in several models with non-Abelian flavor symmetries [98–102]. Such physics can be observed indirectly in the low energy experiments like lepton flavor violating (LFV) processes [74].

The vacuum expectation value (VEV) of the modulus τ plays an important role in modular flavor symmetry, in particular realization of quark and lepton masses and their mixing angles. The modulus VEV is fixed as the potential minimum of the modulus potential, so called the modulus stabilization in modular flavor models [80, 86, 88, 89]. At such a minimum, the F-term of the modulus F^τ may be non-vanishing, and leads to SUSY breaking, that is the moduli-mediated SUSY breaking [103–106]. This specific pattern of soft SUSY breaking terms has been discussed in the LFV [74].

On the other hand, the modular invariance has been also studied in the framework of the generalized CP symmetry [107], which is the non-trivial CP transformation in the non-Abelian discrete flavor symmetry [108–113]. A viable CP invariant lepton model was proposed in the modular A_4 symmetry [68], in which the CP symmetry is broken by fixing τ , that is, the breaking of the modular symmetry (see also [69]). The phenomenological implication of those models were studied by focusing the Pontecorvo-Maki-Nakagawa-Sakata (PMNS) mixing angles [114, 115] and the CP violating Dirac phase of leptons. In this framework, a fixed τ also causes the CP violation in the soft SUSY breaking terms. The electric dipole moments (EDMs) of charged leptons arise from the CP non-conserved soft SUSY breaking terms. The current experimental upper bound of the electron EDM, $|d_e/e| \leq 1.1 \times 10^{-29}$ cm at 90% confidence level has been reported by the ACME Collaboration [116], and the future sensitivity is expected to reach up to $|d_e/e| \simeq 10^{-30}$ cm [117, 118]. This future sensitivity put forward the theoretical studies of some models [119, 120].

In our work, we discuss the electron EDM in the framework of the supersymmetric modular invariant theory of flavors. We take the level 3 finite modular groups, Γ_3 for the flavor symmetry since the property of A_4 flavor symmetry has been well known [121–127]. Indeed, viable CP invariant lepton

models have been investigated linking to the leptogenesis recently [128]. In this flavor symmetry, we study the electron EDM by fixing τ in the soft SUSY breaking term while the observed lepton masses and PMNS mixing angles are completely reproduced. The SUSY mass scale is also significantly constrained [74] by inputting the observed upper bound of LFV, that is the $\mu \rightarrow e\gamma$ decay [129]. In order to see the effect of CP phase in the modulus τ , we examine the correlation between the electron EDM and the decay rate of the $\mu \rightarrow e\gamma$ decay. The correlation is clearly seen by putting the SUSY mass parameters. That is contrast to the case of the conventional non-abelian discrete flavor symmetric model [102, 130, 131]. Indeed, our mass insertion parameters are obtained without uncertainty once the lepton mass matrices and the SUSY mass scale are fixed.

The paper is organized as follows. In section 2, we give a brief review on the CP transformation in the modular symmetry. In section 3, we present the soft SUSY breaking terms in the modular flavor models. In section 4, we present the CP invariant lepton mass matrix in the A_4 modular symmetry. In section 5, we present formulae for the electron EDM and the branching ratio of the $\mu \rightarrow e\gamma$ decay in terms of the soft SUSY breaking masses. In section 6, we present the numerical result of the electron EDM as well as the branching ratio of the $\mu \rightarrow e\gamma$ decay. Section 7 is devoted to the summary. In Appendices A and B, we give the tensor product of the A_4 group and the modular forms, respectively. In Appendices C and D, we present the relevant renormalization group equations (RGEs) and loop functions, respectively. In Appendix E, we show the charged lepton mass matrix with only weight 2 modular forms and corresponding slepton mass matrix.

2 CP transformation in modular symmetry

2.1 Generalized CP symmetry

The CP transformation is non-trivial if the non-Abelian discrete flavor symmetry G is set in the Yukawa sector of a Lagrangian [113, 132]. Let us consider the chiral superfields. The CP is a discrete symmetry which involves both Hermitian conjugation of a chiral superfield $\psi(x)$ and inversion of spatial coordinates,

$$\psi(x) \rightarrow \mathbf{X}_{\mathbf{r}} \bar{\psi}(x_P) , \quad (1)$$

where $x_P = (t, -\mathbf{x})$ and $\mathbf{X}_{\mathbf{r}}$ is a unitary transformation of $\psi(x)$ in the irreducible representation \mathbf{r} of the discrete flavor symmetry G . This transformation is called a generalized CP transformation. If $\mathbf{X}_{\mathbf{r}}$ is the unit matrix, the CP transformation is the trivial one. This is the case for the continuous flavor symmetry [132]. However, in the framework of the non-Abelian discrete family symmetry, non-trivial choices of $\mathbf{X}_{\mathbf{r}}$ are possible. The unbroken CP transformations of $\mathbf{X}_{\mathbf{r}}$ form the group H_{CP} . Then, $\mathbf{X}_{\mathbf{r}}$ must be consistent with the flavor symmetry transformation,

$$\psi(x) \rightarrow \rho_{\mathbf{r}}(g)\psi(x) , \quad g \in G , \quad (2)$$

where $\rho_{\mathbf{r}}(g)$ is the representation matrix for g in the irreducible representation \mathbf{r} .

The condition, which has to be respected for consistent implementation of a generalized CP symmetry along with a flavor symmetry, is given as follows [133–135]:

$$\mathbf{X}_{\mathbf{r}} \rho_{\mathbf{r}}^*(g) \mathbf{X}_{\mathbf{r}}^{-1} = \rho_{\mathbf{r}}(g') , \quad g, g' \in G . \quad (3)$$

This is called the consistency condition for $\mathbf{X}_{\mathbf{r}}$.

2.2 Modular symmetry

The modular group $\bar{\Gamma}$ is the group of linear fractional transformations γ acting on the modulus τ , belonging to the upper-half complex plane as:

$$\tau \longrightarrow \gamma\tau = \frac{a\tau + b}{c\tau + d}, \quad \text{where } a, b, c, d \in \mathbb{Z} \text{ and } ad - bc = 1, \quad \text{Im}[\tau] > 0, \quad (4)$$

which is isomorphic to $PSL(2, \mathbb{Z}) = SL(2, \mathbb{Z})/\{I, -I\}$ transformation. This modular transformation is generated by S and T ,

$$S : \tau \longrightarrow -\frac{1}{\tau}, \quad T : \tau \longrightarrow \tau + 1, \quad (5)$$

which satisfy the following algebraic relations,

$$S^2 = \mathbb{1}, \quad (ST)^3 = \mathbb{1}. \quad (6)$$

We introduce the series of groups $\Gamma(N)$, called principal congruence subgroups, where N is the level $1, 2, 3, \dots$. These groups are defined by

$$\Gamma(N) = \left\{ \begin{pmatrix} a & b \\ c & d \end{pmatrix} \in SL(2, \mathbb{Z}), \quad \begin{pmatrix} a & b \\ c & d \end{pmatrix} = \begin{pmatrix} 1 & 0 \\ 0 & 1 \end{pmatrix} \pmod{N} \right\}. \quad (7)$$

For $N = 2$, we define $\bar{\Gamma}(2) \equiv \Gamma(2)/\{I, -I\}$. Since the element $-I$ does not belong to $\Gamma(N)$ for $N > 2$, we have $\bar{\Gamma}(N) = \Gamma(N)$. The quotient groups defined as $\Gamma_N \equiv \bar{\Gamma}/\bar{\Gamma}(N)$ are finite modular groups. In these finite groups Γ_N , $T^N = \mathbb{1}$ is imposed. The groups Γ_N with $N = 2, 3, 4, 5$ are isomorphic to S_3 , A_4 , S_4 and A_5 , respectively [12].

Modular forms $f_i(\tau)$ of weight k are the holomorphic functions of τ and transform as

$$f_i(\tau) \longrightarrow (c\tau + d)^k \rho(\gamma)_{ij} f_j(\tau), \quad \gamma \in \bar{\Gamma}, \quad (8)$$

under the modular symmetry, where $\rho(\gamma)_{ij}$ is a unitary matrix under Γ_N .

Under the modular transformation of Eq. (4), chiral superfields ψ_i (i denotes flavors) with weight $-k$ transform as [136],

$$\psi_i \longrightarrow (c\tau + d)^{-k} \rho(\gamma)_{ij} \psi_j. \quad (9)$$

We study global SUSY models. The superpotential which is built from matter fields and modular forms is assumed to be modular invariant, i.e., to have a vanishing modular weight. For given modular forms this can be achieved by assigning appropriate weights to the matter superfields.

The kinetic terms are derived from a Kähler potential. The Kähler potential of chiral matter fields ψ_i with the modular weight $-k$ is given simply by

$$\frac{1}{[i(\bar{\tau} - \tau)]^k} \sum_i |\psi_i|^2, \quad (10)$$

where the superfield and its scalar component are denoted by the same letter, and $\bar{\tau} = \tau^*$ after taking VEV of τ . The canonical form of the kinetic terms is obtained by changing the normalization of parameters [17]. The general Kähler potential consistent with the modular symmetry possibly contains additional terms [137]. However, we consider only the simplest form of the Kähler potential.

For $\Gamma_3 \simeq A_4$, the dimension of the linear space $\mathcal{M}_k(\Gamma(3))$ of modular forms of weight k is $k + 1$ [138–140], i.e., there are three linearly independent modular forms of the lowest non-trivial weight 2, which form a triplet of the A_4 group, $Y_3^{(2)}(\tau) = (Y_1(\tau), Y_2(\tau), Y_3(\tau))^T$. These modular forms have been explicitly given [11] in the symmetric base of the A_4 generators S and T for the triplet representation (see Appendix A) in Appendix B.

2.3 CP transformation of the modulus τ and modular multiplets

The CP transformation in the modular symmetry was discussed by using the generalized CP symmetry in Ref. [107]. The CP transformation of the modulus τ is well defined as:

$$\tau \xrightarrow{CP} -\tau^*. \quad (11)$$

The CP transformation of modular forms were given in Ref. [107] as follows. Define a modular multiplet of the irreducible representation \mathbf{r} of Γ_N with weight k as $\mathbf{Y}_{\mathbf{r}}^{(k)}(\tau)$, which is transformed as:

$$\mathbf{Y}_{\mathbf{r}}^{(k)}(\tau) \xrightarrow{CP} \mathbf{Y}_{\mathbf{r}}^{(k)}(-\tau^*), \quad (12)$$

under the CP transformation. The complex conjugated CP transformed modular forms $\mathbf{Y}_{\mathbf{r}}^{(k)*}(-\tau^*)$ transform almost like the original multiplets $\mathbf{Y}_{\mathbf{r}}^{(k)}(\tau)$ under a modular transformation, namely:

$$\mathbf{Y}_{\mathbf{r}}^{(k)*}(-\tau^*) \xrightarrow{\gamma} \mathbf{Y}_{\mathbf{r}}^{(k)*}(-(\gamma\tau)^*) = (c\tau + d)^k \rho_{\mathbf{r}}^*(u(\gamma)) \mathbf{Y}_{\mathbf{r}}^{(k)*}(-\tau^*), \quad (13)$$

where $u(\gamma) \equiv CP\gamma CP^{-1}$ ¹. Using the consistency condition of Eq. (3), which gives $\mathbf{X}_{\mathbf{r}}^T \rho_{\mathbf{r}}^*(u(\gamma)) = \rho_{\mathbf{r}}(\gamma) \mathbf{X}_{\mathbf{r}}^T$, we obtain

$$\mathbf{X}_{\mathbf{r}}^T \mathbf{Y}_{\mathbf{r}}^{(k)*}(-\tau^*) \xrightarrow{\gamma} (c\tau + d)^k \rho_{\mathbf{r}}(\gamma) \mathbf{X}_{\mathbf{r}}^T \mathbf{Y}_{\mathbf{r}}^{(k)*}(-\tau^*). \quad (14)$$

Therefore, if there exists a unique modular multiplet at a level N , weight k and representation \mathbf{r} , which is satisfied for $N = 2-5$ with weight 2, we can express the modular form $\mathbf{Y}_{\mathbf{r}}^{(k)}(\tau)$ as:

$$\mathbf{Y}_{\mathbf{r}}^{(k)}(\tau) = \kappa \mathbf{X}_{\mathbf{r}}^T \mathbf{Y}_{\mathbf{r}}^{(k)*}(-\tau^*), \quad (15)$$

where κ is a proportional coefficient. Make $\mathbf{Y}_{\mathbf{r}}^{(k)*}(-\tau^*)$ by using Eq. (15) and substitute it for $\mathbf{Y}_{\mathbf{r}}^{(k)*}(-\tau^*)$ in the right hand side of Eq. (15). Then, one obtains $\mathbf{X}_{\mathbf{r}}^* \mathbf{X}_{\mathbf{r}} = |\kappa|^2 \mathbb{1}_{\mathbf{r}}$ since $\mathbf{Y}_{\mathbf{r}}^{(k)}(-(-\tau^*)^*) = \mathbf{Y}_{\mathbf{r}}^{(k)}(\tau)$. Therefore, the unitary matrix $\mathbf{X}_{\mathbf{r}}$ is symmetric one, and $\kappa = e^{i\phi}$ is a phase, which can be absorbed in the normalization of modular forms. Thus, the modular symmetry restricts $\mathbf{X}_{\mathbf{r}}$ being symmetric. In conclusion, the CP transformation of modular forms is given as:

$$\mathbf{Y}_{\mathbf{r}}^{(k)}(\tau) \xrightarrow{CP} \mathbf{Y}_{\mathbf{r}}^{(k)}(-\tau^*) = \mathbf{X}_{\mathbf{r}} \mathbf{Y}_{\mathbf{r}}^{(k)*}(\tau). \quad (16)$$

It is also emphasized that $\mathbf{X}_{\mathbf{r}} = \mathbb{1}_{\mathbf{r}}$ satisfies the consistency condition Eq. (3) in a basis that generators of S and T of Γ_N are represented by symmetric matrices because of $\rho_{\mathbf{r}}^*(S) = \rho_{\mathbf{r}}^\dagger(S) = \rho_{\mathbf{r}}(S^{-1}) = \rho_{\mathbf{r}}(S)$ and $\rho_{\mathbf{r}}^*(T) = \rho_{\mathbf{r}}^\dagger(T) = \rho_{\mathbf{r}}(T^{-1})$. Our basis of A_4 generators of Eq. (63) is symmetric one in Appendix A.

The CP transformations of chiral superfields and modular multiplets are summarized as follows:

$$\tau \xrightarrow{CP} -\tau^*, \quad \psi(x) \xrightarrow{CP} \mathbf{X}_{\mathbf{r}} \bar{\psi}(x_P), \quad \mathbf{Y}_{\mathbf{r}}^{(k)}(\tau) \xrightarrow{CP} \mathbf{Y}_{\mathbf{r}}^{(k)}(-\tau^*) = \mathbf{X}_{\mathbf{r}} \mathbf{Y}_{\mathbf{r}}^{(k)*}(\tau), \quad (17)$$

where $\mathbf{X}_{\mathbf{r}} = \mathbb{1}_{\mathbf{r}}$ can be taken in the basis of symmetric generators of S and T . We use this CP transformation of modular forms with $\mathbf{X}_{\mathbf{r}} = \mathbb{1}_{\mathbf{r}}$ to construct the CP invariant lepton mass matrices in section 4.

¹ u acts on the generator as $u(S) = S$ and $u(T) = T^{-1}$ [107].

3 Soft SUSY breaking terms

Let us consider the moduli-mediated SUSY breaking [103–106]. We present the soft SUSY breaking terms due to the modulus F-term, using the unit $M_P = 1$, where M_P denotes the reduced Planck scale. In supergravity theory, the action is given by the Kähler potential K , the superpotential W and the gauge kinetic function f . The kinetic terms are derived from a Kähler potential.

The Kähler potential of chiral matter fields ψ_i with the modular weight $-k_i$ is given simply by

$$K^{\text{matter}} = K_{i\bar{i}} |\psi_i|^2, \quad K_{i\bar{i}} = \frac{1}{[i(\bar{\tau} - \tau)]^{k_i}}. \quad (18)$$

Then, the full Kähler potential is given as:

$$\begin{aligned} K &= K_0(\tau, M) + K^{\text{matter}}, \\ K_0(\tau, M) &= -\ln(i(\bar{\tau} - \tau)) + K(M, \bar{M}), \end{aligned} \quad (19)$$

where M denotes moduli other than τ .

The superpotential W is given as:

$$W = Y_{ijk}(\tau) \Phi_i \Phi_j \Phi_k + M_{ij}(\tau) \Phi_i \Phi_j \cdots. \quad (20)$$

We suppose that the gauge kinetic function is independent of the modulus τ , i.e. $f(M)$ since the modulus τ does not appear in the gauge kinetic function at tree level.

Let us consider the case that the SUSY breaking occurs by some F-terms of moduli X , F^X ($F^X \neq 0$). The canonical form of the kinetic terms is obtained by changing the normalization of parameters. In the canonical normalization, the soft masses \tilde{m}_i and the A-term are given as [103]:

$$\tilde{m}_i^2 = m_{3/2}^2 - \sum_X |F^X|^2 \partial_X \partial_{\bar{X}} \ln K_{i\bar{i}}, \quad (21)$$

and

$$\begin{aligned} A_{ijk} &= A_i + A_j + A_k - \sum_X \frac{F^X}{Y_{ijk}} \partial_X Y_{ijk}, \\ A_i &= \sum_X F^X \partial_X \ln e^{-K_0/3} K_{i\bar{i}}, \end{aligned} \quad (22)$$

where i, j and k denote flavors. Here, Yukawa couplings \tilde{Y}_{ijk} in global SUSY superpotential are related with Yukawa couplings Y_{ijk} in the supergravity superpotential as follows:

$$|\tilde{Y}_{ijk}|^2 = e^{K_0} |Y_{ijk}|^2. \quad (23)$$

That is, the global SUSY superpotential has vanishing modular weight while the supergravity superpotential has the modular weight -1 . Our modular flavor model is studied in global SUSY basis.

Suppose the case of $X = \tau$. The Kähler potential K in Eq. (19) leads to the soft mass

$$\tilde{m}_i^2 = m_{3/2}^2 - k_i \frac{|F^\tau|^2}{(2 \operatorname{Im} \tau)^2}, \quad (24)$$

where $m_{3/2}$ is the gravitino mass. It is remarked that \tilde{m}_i^2 becomes tachyonic if $k_i|F^\tau|^2/(2\text{Im}\tau)^2$ is larger than $m_{3/2}^2$. Since \tilde{m}_i should be at least larger than $\mathcal{O}(1)$ TeV, Eq. (24) provides a significant constraint with our phenomenological discussion.

On the other hand, the A-term is written by

$$\begin{aligned} A_{ijk} &= A_{ijk}^0 + A'_{ijk}, \\ A_{ijk}^0 &= (1 - k_i - k_j - k_k) \frac{F^\tau}{2\text{Im}\tau}, \quad A'_{ijk} = \frac{F^\tau}{Y_{ijk}} \frac{dY_{ijk}(\tau)}{d\tau}. \end{aligned} \quad (25)$$

Then, we have the soft mass term $h_{ijk} = Y_{ijk}A_{ijk}$. Note that in our convention τ is dimensionless, and F^τ has dimension one. Gaugino masses can be generated by F-terms of other moduli, F^M , while F^τ has universal contributions on soft masses and A-terms.

If we have common weights for three generations in the modular flavor model, the soft mass \tilde{m}_i is flavor blind. Then, the left-handed and right-handed slepton mass matrices \tilde{m}_{eLi} and \tilde{m}_{eRi} are universal as:

$$\tilde{m}_{eLi}^2 = \tilde{m}_{eL0}^2, \quad \tilde{m}_{eRi}^2 = \tilde{m}_{eR0}^2, \quad (26)$$

that is, they are proportional to the unit matrix, which does not contribute the LFV. This is the case in the previous study of Ref. [74]. However, the condition of the universal slepton masses is relaxed in our phenomenological discussion by the assignment of different weights for the three right-handed charged leptons. Non-universal slepton mass matrices contribute to the LFV.

The first term of A_{ijk} term of Eq. (25) A_{ijk}^0 also contributes to the LFV in addition to the second term A'_{ijk} in the case of different weights for the three right-handed charged leptons.

4 CP invariant lepton model in A_4 modular symmetry

4.1 Lepton mass matrices

The CP invariant lepton mass matrices have been proposed in the A_4 modular symmetry [68, 128]. We adopt those ones in order to discuss the soft SUSY breaking terms. The three generations of the left-handed lepton doublets are assigned to be an A_4 triplet L , and the right-handed charged leptons e^c , μ^c , and τ^c are A_4 singlets $\mathbf{1}$, $\mathbf{1}''$ and $\mathbf{1}'$, respectively. The three generations of the right-handed Majorana neutrinos are also assigned to be an A_4 triplet N^c [128]. The weight of the superfields of left-handed leptons is fixed to be 1 as a reference value. The weight of right-handed neutrinos is also taken to be 1 in order to give a Dirac neutrino mass matrix in terms of modular forms of weight 2. On the other hand, weights of the right-handed charged leptons e^c , μ^c and τ^c are put (k_e, k_μ, k_τ) . Weights of Higgs fields H_u , H_d are fixed to be 0. The representations and weights for MSSM fields and modular forms of weight k are summarized in Table 1.

	L	(e^c, μ^c, τ^c)	N^c	H_u	H_d	$Y_3^{(k)}$
$SU(2)$	2	1	1	2	2	1
A_4	3	(1, 1'', 1')	3	1	1	3
weight	1	(k_e, k_μ, k_τ)	1	0	0	k

Table 1: Representations and weights for superfields and relevant modular forms of weight k .

At first, we present the neutrino mass matrices. In Table 1, the A_4 invariant superpotential for the neutrino sector, w_ν , is given as:

$$\begin{aligned} w_\nu &= w_D + w_N, \\ w_D &= \gamma_\nu N^c H_u Y_{\mathbf{3}}^{(2)} L + \gamma'_\nu N^c H_u Y_{\mathbf{3}}^{(2)} L, \\ w_N &= \Lambda N^c N^c Y_{\mathbf{3}}^{(2)}, \end{aligned} \quad (27)$$

where γ_ν and γ'_ν are Yukawa couplings, and Λ denotes a right-handed Majorana neutrino mass scale. By putting v_u for VEV of the neutral component of H_u and taking a triplet $(\nu_e, \nu_\mu, \nu_\tau)$ for neutrinos, the Dirac neutrino mass matrix, M_D , is obtained as

$$M_D = \gamma_\nu v_u \begin{pmatrix} 2Y_1 & (-1 + g_D)Y_3 & (-1 - g_D)Y_2 \\ (-1 - g_D)Y_3 & 2Y_2 & (-1 + g_D)Y_1 \\ (-1 + g_D)Y_2 & (-1 - g_D)Y_1 & 2Y_3 \end{pmatrix}_{RL}, \quad (28)$$

where $g_D = \gamma'_\nu / \gamma_\nu$. On the other hand the right-handed Majorana neutrino mass matrix, M_N is written as follows:

$$M_N = \Lambda \begin{pmatrix} 2Y_1 & -Y_3 & -Y_2 \\ -Y_3 & 2Y_2 & -Y_1 \\ -Y_2 & -Y_1 & 2Y_3 \end{pmatrix}_{RR}. \quad (29)$$

By using the type-I seesaw mechanism, the effective neutrino mass matrix, M_ν is obtained as

$$M_\nu = M_D^T M_N^{-1} M_D. \quad (30)$$

We propose the charged lepton mass matrices with minimum number of parameters to reproduce the observed lepton masses and PMNS mixing angles. Indeed, there are four choices of weights right-handed charged leptons, those are $(k_e = 1, k_\mu = 1, k_\tau = 5)$, $(k_e = 1, k_\mu = 3, k_\tau = 5)$, $(k_e = 1, k_\mu = 1, k_\tau = 7)$ and $(k_e = 1, k_\mu = 3, k_\tau = 7)$ labeled as cases A, B, C and D, respectively in our numerical study, as will be discussed later. Then, we need modular forms of weight 2, 4, 6 and 8, which are presented in Appendix B.

Then, the A_4 invariant superpotential of the charged leptons, w_e , by taking into account the modular weights is obtained as

$$w_e = \alpha_e e^c H_d Y_{\mathbf{3}}^{(2)} L + \beta_e \mu^c H_d Y_{\mathbf{3}}^{(k_\mu+1)} L + \gamma_e \tau^c H_d Y_{\mathbf{3}}^{(k_\tau+1)} L + \gamma'_e \tau^c H_d Y_{\mathbf{3}'}^{(k_\tau+1)} L, \quad (31)$$

where α_e , β_e , γ_e , and γ'_e are constant parameters. Under CP, the superfields transform as:

$$e^c \xrightarrow{CP} X_1^* \bar{e}^c, \quad \mu^c \xrightarrow{CP} X_{1''}^* \bar{\mu}^c, \quad \tau^c \xrightarrow{CP} X_{1'}^* \bar{\tau}^c, \quad L \xrightarrow{CP} X_3 \bar{L}, \quad H_d \xrightarrow{CP} \eta_d \bar{H}_d, \quad (32)$$

and we can take $\eta_d = 1$ without loss of generality. Since the representations of S and T are symmetric (see Appendix A), we can choose $X_{\mathbf{3}} = \mathbf{1}_{\mathbf{3}}$ and $X_{\mathbf{1}} = X_{1'} = X_{1''} = \mathbf{1}$ as discussed in Eq. (17).

Taking a triplet (e_L, μ_L, τ_L) in the flavor base, the charged lepton mass matrix M_E is simply written as:

$$M_E(\tau) = v_d \begin{pmatrix} \alpha_e & 0 & 0 \\ 0 & \beta_e & 0 \\ 0 & 0 & \gamma_e \end{pmatrix} \begin{pmatrix} Y_1^{(2)}(\tau) & Y_3^{(2)}(\tau) & Y_2^{(2)}(\tau) \\ Y_2^{(m)}(\tau) & Y_1^{(m)}(\tau) & Y_3^{(m)}(\tau) \\ Y_3^{(n)}(\tau) + g_e Y_3'^{(n)}(\tau) & Y_2^{(n)}(\tau) + g_e Y_2'^{(n)}(\tau) & Y_1^{(n)}(\tau) + g_e Y_1'^{(n)}(\tau) \end{pmatrix}, \quad (33)$$

where $m = k_\mu + 1$ and $n = k_\tau + 1$ for weights of modular forms in our case. The new parameter g_e is defined as $g_e = \gamma'_e/\gamma_e$ and v_d is VEV of the neutral component of H_d . The coefficients α_e , β_e and γ_e are taken to be real without loss of generality. Under CP transformation, the mass matrix M_E is transformed following from Eq. (33) as:

$$M_e(\tau) \xrightarrow{CP} M_e(-\tau^*) = M_e^*(\tau) = v_d \begin{pmatrix} \alpha_e & 0 & 0 \\ 0 & \beta_e & 0 \\ 0 & 0 & \gamma_e \end{pmatrix} \begin{pmatrix} Y_1^{(2)}(\tau)^* & Y_3^{(2)}(\tau)^* & Y_2^{(2)}(\tau)^* \\ Y_2^{(m)}(\tau)^* & Y_1^{(m)}(\tau)^* & Y_3^{(m)}(\tau)^* \\ Y_3^{(n)}(\tau)^* + g_e^* Y_3'^{(n)}(\tau)^* & Y_2^{(n)}(\tau)^* + g_e^* Y_2'^{(n)}(\tau)^* & Y_1^{(n)}(\tau)^* + g_e^* Y_1'^{(n)}(\tau)^* \end{pmatrix}. \quad (34)$$

In a CP conserving modular invariant theory, both CP and modular symmetries are broken spontaneously by VEV of the modulus τ . However, there exists certain values of τ which conserve CP while breaking the modular symmetry. Obviously, this is the case if τ is left invariant by CP, i.e.

$$\tau \xrightarrow{CP} -\tau^* = \tau, \quad (35)$$

which indicates τ lies on the imaginary axis, $\text{Re}[\tau] = 0$. In addition to $\text{Re}[\tau] = 0$, CP is conserved at the boundary of the fundamental domain.

Due to Eq. (17), one then has

$$M_\nu(\tau) = M_\nu^*(\tau), \quad M_e(\tau) = M_e^*(\tau), \quad (36)$$

if g_e and g_D are taken to be real. Therefore, the source of the CP violation is only non-trivial $\text{Re}[\tau]$ after breaking the modular symmetry. Numerical results of the CP violation have been obtained by fixing the modulus τ with real g_e and g_D .

4.2 Soft masses of sleptons

As presented in section 3, the SUSY breaking due to the modulus F term gives the soft mass terms of sleptons, \tilde{m}_L^2 , \tilde{m}_R^2 and \tilde{m}_{RL}^2 as:

$$\begin{aligned} (\tilde{m}_{eR}^2)_{ii} &= m_{3/2}^2 - k_i \frac{|F^\tau|^2}{(2 \text{Im } \tau)^2}, & (\tilde{m}_{eL}^2)_{jj} &= m_{3/2}^2 - k_j \frac{|F^\tau|^2}{(2 \text{Im } \tau)^2}, \\ (\tilde{m}_{eRL}^2)_{ij} &\equiv v_d h_{ijk} = v_d (1 - k_i - k_j) \frac{F^\tau}{2 \text{Im } \tau} Y_{ij} + v_d F^\tau \frac{dY_{ij}(\tau)}{d\tau}, \end{aligned} \quad (37)$$

where i, j denote the right-handed and left-handed flavors and the subscript index k is omitted in h_{ijk} , and the weight of Higgs fields k_k in Eq. (25) is set to be *zero* without loss of generality. The subscript indices L and R refer to the chirality of the corresponding SM leptons. The Yukawa matrix Y_{ij} is given by the charged lepton mass matrix in Eq.(33) of subsection 4.1 as M_E/v_d . Slepton mass matrices \tilde{m}_{eL}^2 and \tilde{m}_{eR}^2 are diagonal matrices, on the other hand, \tilde{m}_{eRL}^2 has off-diagonal entries in the present flavor basis². It is noted that the mass term \tilde{m}_{eLR}^2 is given by \tilde{m}_{eRL}^2 [†].

Let take the models in subsection 4.1, where weights of three right-handed charged leptons are k_e , k_μ and k_τ , respectively. On the other hand, k_j of weights for left-handed leptons are universal as 1, because left-handed leptons are constituents of a A_4 triplet.

²The SUSY sector of neutrinos is neglected since the right-handed Majorana neutrinos decouples at the high energy scale in our model. The effect of the right-handed neutrinos is discuss in section 6.

The soft masses of L and R are given:

$$\tilde{m}_{eL}^2 = \begin{pmatrix} m_{3/2}^2 - |m_F|^2 & 0 & 0 \\ 0 & m_{3/2}^2 - |m_F|^2 & 0 \\ 0 & 0 & m_{3/2}^2 - |m_F|^2 \end{pmatrix}, \quad (38)$$

$$\tilde{m}_{eR}^2 = \begin{pmatrix} m_{3/2}^2 - k_e |m_F|^2 & 0 & 0 \\ 0 & m_{3/2}^2 - k_\mu |m_F|^2 & 0 \\ 0 & 0 & m_{3/2}^2 - k_\tau |m_F|^2 \end{pmatrix}, \quad (39)$$

$$(40)$$

where

$$m_F = \frac{F^\tau}{2 \operatorname{Im} \tau}. \quad (41)$$

Thus, \tilde{m}_{eL}^2 matrix is universal for flavors (proportional to unit matrix), but \tilde{m}_{eR}^2 one is not universal in our models. Therefore, after moving to the super-PMNS base (diagonal base of the neutrino and charged leptons), the off-diagonal entries of \tilde{m}_{eR}^2 appear, but the off-diagonal entries of \tilde{m}_{eL}^2 are not induced³.

As discussed in Eq. (24), the slepton masses become tachyonic if $k_i |F^\tau|^2 / (2 \operatorname{Im} \tau)^2$ is larger than $m_{3/2}^2$. Therefore, the magnitude of F^τ is significantly constrained for the larger weight k_i in our phenomenological discussion.

The \tilde{m}_{eRL}^2 matrix has a different flavor structure, which is shown as:

$$\begin{aligned} \tilde{m}_{eRL}^2 &\simeq v_d \times \\ &\left[m_F \begin{pmatrix} -k_e \alpha_e & 0 & 0 \\ 0 & -k_\mu \beta_e & 0 \\ 0 & 0 & -k_\tau \gamma_e \end{pmatrix} \begin{pmatrix} Y_1^{(2)} & Y_3^{(2)} & Y_2^{(2)} \\ Y_2^{(m)} & Y_1^{(m)} & Y_3^{(m)} \\ Y_3^{(n)} + g_e Y_3'^{(n)} & Y_2^{(n)} + g_e Y_2'^{(n)} & Y_1^{(n)} + g_e Y_1'^{(n)} \end{pmatrix} \right. \\ &\quad \left. + F^\tau \begin{pmatrix} \alpha_e & 0 & 0 \\ 0 & \beta_e & 0 \\ 0 & 0 & \gamma_e \end{pmatrix} \frac{d}{d\tau} \begin{pmatrix} Y_1^{(2)} & Y_3^{(2)} & Y_2^{(2)} \\ Y_2^{(m)} & Y_1^{(m)} & Y_3^{(m)} \\ Y_3^{(n)} + g_e Y_3'^{(n)} & Y_2^{(n)} + g_e Y_2'^{(n)} & Y_1^{(n)} + g_e Y_1'^{(n)} \end{pmatrix} \right], \quad (42) \end{aligned}$$

where $m = 2$ or 4 , and $n = 6$ or 8 for weights of modular forms in our models. The second term of right-hand side in Eq. (42) is the derivative of the modular forms with respect to the modulus τ .

The parameters in these slepton mass matrices, $m_{3/2}$ and F^τ are taken to be real to give the CP conserving modular invariant model. The CP violation is caused by fixing τ in the soft mass terms as well as in the lepton mass matrices. We also suppose real gaugino masses.

In order to study the phenomenological implications of the soft SUSY breaking sector, we rotate these slepton mass matrices into the physical basis where the Yukawa matrices are real diagonal

³We neglect RGE effects from Yukawa couplings of leptons since they are very small at $\tan \beta \simeq 5$, which is used in the numerical calculations of section 6.

and positive, i.e. the super-PMNS basis. Any misalignment between the lepton and slepton flavor matrices gives a source of CP violation and LFV in the low-energy phenomena.

With these soft masses, the amount of flavor violation can be addressed in terms of the dimensionless mass insertion parameters. We adopt the definition in Ref. [102] for mass insertion parameters because slepton masses are not universal for flavors. The (i, j) elements of mass insertion parameters are given as:

$$(\delta_{eLL})_{ij} = \frac{(\tilde{m}_{eL}^2)_{ij}}{\langle \tilde{m}_e \rangle_{LL}^2}, \quad (\delta_{eRR})_{ij} = \frac{(\tilde{m}_{eR}^2)_{ij}}{\langle \tilde{m}_e \rangle_{RR}^2}, \quad (\delta_{eLR})_{ij} = \frac{(\tilde{m}_{eLR}^2)_{ij}}{\langle \tilde{m}_e \rangle_{LR}^2}, \quad (\delta_{eRL})_{ij} = \frac{(\tilde{m}_{eRL}^2)_{ij}}{\langle \tilde{m}_e \rangle_{RL}^2}, \quad (43)$$

where the averaged masses in the denominators are defined by

$$\langle \tilde{m}_e \rangle_{AB}^2 = \sqrt{(\tilde{m}_{eA}^2)_{ii} (\tilde{m}_{eB}^2)_{jj}}. \quad (44)$$

By using these parameters, we discuss the phenomenological implication of our modular invariant models.

4.3 RGEs effect of sleptons

Our model of leptons are set at the high energy Q_0 . Therefore, we take into account the running effects of slepton mass matrices at the low energy scale Q . The renormalization group equations (RGEs) are shown in Appendix C. Since Yukawa couplings of charged leptons are small, the evolutions of off-diagonal elements are dominated by the gauge couplings. Thus, the largest contributions of the RGEs evolution for off-diagonal elements of A-term is flavor independent. Then, we can estimate the running effects by [101, 141, 142]

$$A_{eij}(Q) \simeq \exp \left[\frac{-1}{16\pi^2} \int_{Q_0}^Q dt \left(\frac{9}{5} g_1^2 + 3g_2^2 \right) \right] A_{eij}(m_{\text{GUT}}) \approx 1.4 \times A_{eij}(Q_0), \quad (45)$$

where $g_{1,2}$ are the gauge couplings of $\text{SU}(2)_L \times U(1)_Y$ and $t = \ln Q/Q_0$. Numerical coefficient 1.4 is obtained by taking $Q_0 = 10^{16} \text{ GeV}$ and $Q = 1 \text{ TeV}$ for a reference.

Therefore, the mass term \tilde{m}_{eRL}^2 is given as

$$\begin{aligned} \tilde{m}_{eRL}^2 &\simeq 1.4 v_d \times \\ &\left[m_F \begin{pmatrix} -k_e \alpha_e & 0 & 0 \\ 0 & -k_\mu \beta_e & 0 \\ 0 & 0 & -k_\tau \gamma_e \end{pmatrix} \begin{pmatrix} Y_1^{(2)} & Y_3^{(2)} & Y_2^{(2)} \\ Y_2^{(m)} & Y_1^{(m)} & Y_3^{(m)} \\ Y_3^{(n)} + g_e Y_3'^{(n)} & Y_2^{(n)} + g_e Y_2'^{(n)} & Y_1^{(n)} + g_e Y_1'^{(n)} \end{pmatrix} \right. \\ &\left. + F^\tau \begin{pmatrix} \alpha_e & 0 & 0 \\ 0 & \beta_e & 0 \\ 0 & 0 & \gamma_e \end{pmatrix} \frac{d}{d\tau} \begin{pmatrix} Y_1^{(2)} & Y_3^{(2)} & Y_2^{(2)} \\ Y_2^{(m)} & Y_1^{(m)} & Y_3^{(m)} \\ Y_3^{(n)} + g_e Y_3'^{(n)} & Y_2^{(n)} + g_e Y_2'^{(n)} & Y_1^{(n)} + g_e Y_1'^{(n)} \end{pmatrix} \right], \quad (46) \end{aligned}$$

where $m = 2$ or 4 , and $n = 6$ or 8 for weights of modular forms.

In the supergravity framework, soft masses for all scalar particles have the common scale denoted by m_0 , and gauginos also have the common scale $M_{1/2}$. Therefore, at Q_0 , we take real masses as:

$$M_1(Q_0) = M_2(Q_0) = M_{1/2}, \quad (47)$$

where M_1 and M_2 are the bino and wino masses, respectively. The effects of RGEs lead at the low energy scale Q to following masses for gauginos [141, 142]

$$M_1(Q) \simeq \frac{\alpha_1(Q)}{\alpha_1(Q_0)} M_1(Q_0), \quad M_2(Q) \simeq \frac{\alpha_2(Q)}{\alpha_2(Q_0)} M_2(Q_0), \quad (48)$$

where $\alpha_i = g_i^2/4\pi$ ($i = 1, 2$) and according to the gauge coupling unification at Q_0 , $\alpha_1(Q_0) = \alpha_2(Q_0) \simeq 1/25$. Then, the low energy gaugino masses

$$M_1 \approx 0.49 M_{1/2}, \quad M_2 \approx 0.86 M_{1/2}, \quad (49)$$

by taking $Q_0 = 10^{16}$ GeV and $Q = 1$ TeV.

On the other hand, taking into account the RGEs effect on the average mass scale in \tilde{m}_{eL}^2 and \tilde{m}_{eR}^2 , we have [141, 142]

$$\begin{aligned} \tilde{m}_{eL}^2(Q) &\simeq \tilde{m}_{eL}^2(Q_0) + K_2(Q) + \frac{1}{4} K_1(Q), \\ \tilde{m}_{eR}^2(Q) &\simeq \tilde{m}_{eR}^2(Q_0) + K_1(Q), \end{aligned} \quad (50)$$

where

$$K_1(Q) = \frac{3}{5} \frac{1}{2\pi^2} \int_{\ln Q}^{\ln Q_0} dt g_1^2(t) M_1(t)^2, \quad K_2(Q) = \frac{3}{4} \frac{1}{2\pi^2} \int_{\ln Q}^{\ln Q_0} dt g_2^2(t) M_2(t)^2. \quad (51)$$

We neglect the hyperfine splitting $\mathcal{O}(M_Z^2)$ in the slepton mass spectrum produced by electroweak symmetry breaking because of $M_{1/2} \gg M_Z$. We obtain numerically

$$(K_1, K_2) \simeq (0.14 M_{1/2}^2, 0.40 M_{1/2}^2), \quad (52)$$

which are flavor independent. The soft masses of L and R are given as:

$$\begin{aligned} \tilde{m}_{eL}^2 &\simeq \begin{pmatrix} m_0^2 - m_F^2 & 0 & 0 \\ 0 & m_0^2 - m_F^2 & 0 \\ 0 & 0 & m_0^2 - m_F^2 \end{pmatrix} + (0.40 + \frac{0.14}{4}) M_{1/2}^2 \begin{pmatrix} 1 & 0 & 0 \\ 0 & 1 & 0 \\ 0 & 0 & 1 \end{pmatrix}, \\ \tilde{m}_{eR}^2 &\simeq \begin{pmatrix} m_0^2 - k_e m_F^2 & 0 & 0 \\ 0 & m_0^2 - k_\mu m_F^2 & 0 \\ 0 & 0 & m_0^2 - k_\tau m_F^2 \end{pmatrix} + 0.14 M_{1/2}^2 \begin{pmatrix} 1 & 0 & 0 \\ 0 & 1 & 0 \\ 0 & 0 & 1 \end{pmatrix}, \end{aligned} \quad (53)$$

where $m_{3/2} = m_0$ is put.

The parameter μ is given through the requirement of the correct electroweak symmetry breaking [102, 130, 141, 142] :

$$|\mu|^2 = \frac{\tilde{m}_{H_d}^2 - \tilde{m}_{H_u}^2 \tan^2 \beta}{\tan^2 \beta - 1} - \frac{1}{2} m_Z^2. \quad (54)$$

At the low energy, $|\mu|^2$ turns to [130]

$$|\mu|^2 \simeq -\frac{m_Z^2}{2} + m_0^2 \frac{1 + 0.5 \tan^2 \beta}{\tan^2 \beta - 1} + M_{1/2}^2 \frac{0.5 + 3.5 \tan^2 \beta}{\tan^2 \beta - 1}, \quad (55)$$

which is determined by fixing m_0 , $M_{1/2}$ and $\tan \beta$. We also take μ to be real positive.

Our predictions of the electron EDM and the branching ratio of $\mu \rightarrow e\gamma$ are given at the 1 TeV mass scale. The RGE effects of them below 1 TeV are induced by the Yukawa couplings of charged leptons and gauge couplings g_1 and g_2 . We can neglect these RGE effects since the Yukawa couplings of charged leptons are small in our model and there is no QCD couplings in the one-loop level. The gauge coupling contributions below 1 TeV are $\mathcal{O}(1)\%$. This contribution does not affect our numerical results.

5 Electron EDM and $\mu \rightarrow e\gamma$ decay

5.1 Electron EDM

The current experimental limit for the electric dipole moment of the electron is given by ACME collaboration [116]:

$$|d_e| \lesssim 1.1 \times 10^{-29} e \text{ cm}, \quad (56)$$

at 90% confidence level. Precise measurements of the electron EDM are rapidly being updated. The future sensitivity is expected to reach up to $|d_e/e| \simeq 10^{-30} \text{ cm}$ [117, 118]. This bound and future sensitivity can test the framework of the supersymmetric modular invariant theory of flavors. The corresponding EDM formula of leptons is given as [102]:

$$\begin{aligned} \frac{d_e}{e} = & \frac{\alpha_1}{8\pi} \frac{M_1}{\tilde{m}_e^4} \tilde{m}_{eL} \text{Im} \left[-(\delta_{eLR})_{11} C_B(\bar{x}) \tilde{m}_{eR} \right. \\ & + \left\{ (\delta_{eLL})_{1i} (\delta_{eLR})_{i1} C'_{B,L}(\bar{x}) + (\delta_{eLR})_{1i} (\delta_{eRR})_{i1} C'_{B,R}(\bar{x}) \right\} \tilde{m}_{eR_{ii}} \\ & \left. - \left\{ (\delta_{eLL})_{1i} (\delta_{eLR})_{ij} (\delta_{eRR})_{j1} + (\delta_{eLR})_{1j} (\delta_{eRL})_{ji} (\delta_{eLR})_{i1} \right\} C''_B(\bar{x}) \tilde{m}_{eR_{jj}} \right], \end{aligned} \quad (57)$$

where \tilde{m}_{eL} and \tilde{m}_{eR} are first mass eigenvalues of \tilde{m}_{eL}^2 and \tilde{m}_{eR}^2 , respectively, and \tilde{m}_e is the averaged mass of L and R as $\tilde{m}_e = \sqrt{\tilde{m}_{eL} \tilde{m}_{eR}}$. Moreover $\tilde{m}_{eR_{ii}}$ denotes the i -th mass eigenvalue of \tilde{m}_{eR}^2 . The expression of Eq. (57) is proportional to the bino mass M_1 . The dimensionless loop functions $C_B(\bar{x})$ etc. are presented in Appendix D. Since our slepton masses of L and R are not so different each other, we adopt the approximate formulae for $C_B(\bar{x})$, $C''_B(\bar{x})$ and $C'_{B,L}(\bar{x})$ [102] by using $\bar{x} = (M_1/\tilde{m}_e)^2$.

The dominant contribution to the electron EDM comes from the first term of the right-hand side, which is the single chirality flipping diagonal mass insertion $(\delta_{eLR})_{11}$, so called flavor-conserving EDM. Its imaginary part is non-zero due to the VEV of the modulus τ , which allows a non-trivial CP phase in \tilde{m}_{eRL}^2 to be different from the phases of the charged lepton mass matrix. The next-to-leading order term is so called flavored EDM [143], which is related with the FCNC of leptons. We will examine both contribution to the electron EDM.

5.2 Branching ratio of $\mu \rightarrow e\gamma$

Once non-vanishing off-diagonal elements in the slepton mass matrices are generated, LFV rare decays like $\mu \rightarrow e\gamma$ are naturally induced by the one-loop diagrams with the exchange of gauginos and sleptons [144–146]. The branching ratio of $\mu \rightarrow e\gamma$ is given as [102]:

$$\begin{aligned} \text{BR}(\mu \rightarrow e\gamma) &= \alpha_{\text{em}} \frac{3}{2\pi} \tan^4 \theta_W M_W^4 \bar{x} \frac{\mu^2 \tan^2 \beta}{\tilde{m}_e^6} \times \\ &\times \left(\left| (\delta_{eLL})_{12} \left(-(\delta_{eLR})_{22} \frac{\tilde{m}_{eL} \tilde{m}_{eR}}{\mu \tan \beta m_\mu} C'_{B,L} + \frac{1}{2} C'_L + C'_2 \right) + (\delta_{eLR})_{12} \frac{\tilde{m}_{eL} \tilde{m}_{eR}}{\mu \tan \beta m_\mu} C_B \right|^2 \right. \\ &\left. + \left| (\delta_{eRR})_{12} \left(-(\delta_{eLR})_{22}^* \frac{m_{eL} m_{eR}}{\mu \tan \beta m_\mu} C'_{B,R} - C'_R \right) + (\delta_{eLR})_{21}^* \frac{\tilde{m}_{eL} m_{eR}}{\mu \tan \beta m_\mu} C_B \right|^2 \right), \end{aligned} \quad (58)$$

where we put $\sin^2 \theta_W = 0.231$. The dimensionless loop functions are presented in Appendix D. In our model, the leading terms come from $(\delta_{eLR})_{12}$ and $(\delta_{eLR})_{21}^*$ due to the chiral enhancement. The next-to-leading ones arise from $(\delta_{eRR})_{12}$. The off-diagonal component $(\delta_{eLL})_{12}$ does not come out in our model.

In SUSY models, the branching ratio of $\ell_i \rightarrow \ell_j \ell_k \bar{\ell}_k$ and the conversion rate of $\mu N \rightarrow eN$ are related simply as [146]:

$$\frac{\text{BR}(\ell_i \rightarrow \ell_j \ell_k \bar{\ell}_k)}{\text{BR}(\ell_i \rightarrow \ell_j \gamma)} = \frac{\alpha_{\text{em}}}{3\pi} \left(2 \log \frac{m_{\ell_i}}{m_{\ell_k}} - 3 \right), \quad \frac{\text{CR}(\mu N \rightarrow eN)}{\text{BR}(\ell_i \rightarrow \ell_j \gamma)} = \alpha_{\text{em}}, \quad (59)$$

where α_{em} is the electromagnetic fine-structure constant.

Current experimental bounds and future prospects of EDM, $\mu \rightarrow e\gamma$ and relevant processes are summarized in Table 2.

	Current bounds	Future prospects
$ d_e/e \text{ cm}$	1.1×10^{-29} [116]	$\sim 10^{-30}$ [117, 118]
$\text{BR}(\mu \rightarrow e\gamma)$	4.2×10^{-13} [129, 157]	6×10^{-14} [152]
$\text{BR}(\mu \rightarrow ee\bar{e})$	1.0×10^{-12} [157]	$\sim 10^{-16}$ [153–155]
$\text{CR}(\mu N \rightarrow eN)$	7.0×10^{-13} [157]	$\sim 10^{-16}$ [153–155]

Table 2: Current experimental bounds and future prospects of relevant processes.

6 Numerical results

As discussed in subsection 4.1, the CP invariant lepton mass matrices have been given in the A_4 modular symmetry [128]. The tiny neutrino masses are obtained by type-I seesaw. The CP symmetry is broken spontaneously by the VEV of the modulus τ . Thus, the fixed value of τ breaks the CP symmetry as well as the modular invariance. The source of the CP phase is the real part of τ . Lepton mass matrices of four cases of weights (k_e, k_μ, k_τ) are completely consistent with observed lepton masses and PMNS mixing angles. Then, the CP violating Dirac phase is predicted clearly at the fixed value of τ [128]. The predicted CP phases of five cases are different as seen in Table 3.

By using those successful charged lepton mass matrices, we calculate the electron EDM and the branching ratio of $\mu \rightarrow e\gamma$. In our numerical analyses, we take four cases A, B, C and D with weights of right-handed charged leptons (k_e, k_μ, k_τ) :

$$(k_e, k_\mu, k_\tau) : A(1, 1, 5), \quad B(1, 3, 5), \quad C(1, 1, 7), \quad D(1, 3, 7).$$

We also discuss the alternative case E, where the charged lepton mass matrix is written with only weight 2 modular forms, $(k_e, k_\mu, k_\tau) = (1, 1, 1)$ (see Appendix E), in which the branching ratio of $\mu \rightarrow e\gamma$ was studied in Ref. [74]. In the case of E, the neutrino mass matrix is given by the dimension-five Weinberg operator instead of type-I seesaw ⁴.

(k_e, k_μ, k_τ)	A (1, 1, 5)	B (1, 3, 5)	C (1, 1, 7)	D (1, 3, 7)
τ	$-0.1912 + 1.1194i$	$0.1931 + 1.1240i$	$0.0901 + 1.0047i$	$-0.1027 + 1.0050i$
g_D	-0.800	-0.800	-0.660	0.685
g_e	-0.905	-0.900	-0.530	-0.573
β_e/α_e	3.70×10^{-3}	4.73×10^{-3}	5.94×10^{-3}	6.30×10^{-3}
γ_e/α_e	9.71	10.1	17.6	16.0
$\sin^2 \theta_{12}$	0.305	0.309	0.324	0.326
$\sin^2 \theta_{23}$	0.569	0.574	0.441	0.479
$\sin^2 \theta_{13}$	0.0222	0.0225	0.0222	0.0223
δ_{CP}^ℓ	172°	187°	183°	176°
$\sum m_i$	62.5 meV	62.8 meV	60.5 meV	60.7 meV
$\sqrt{\chi^2}$	1.08	1.43	2.16	2.38

Table 3: Numerical values of parameters τ , g_D , g_e , β_e/α_e , γ_e/α_e and output of best fitting three mixing angles. The CP violating Dirac phase δ_{CP}^ℓ and the sum of three neutrino masses $\sum m_i$ are predicted. The square root of the sum of χ^2 are also shown.

In Table 3, we show five parameters of models, out put of three mixing angles and predicted the CP violating Dirac phase and the sum of neutrino masses at the best-fit values for cases A, B, C and D in the normal hierarchy of neutrino masses (NH) ⁵, where neutrino data of NuFit 5.0 are put [149]. The charged lepton masses are fitted at the high energy scale 2×10^{16} GeV with $\tan \beta \equiv v_u/v_d = 5$ [150, 151]. The parameter g_D appears in the neutrino Dirac mass matrix in Eq. (28) and is real as seen in Eq. (36). Since we discuss sleptons, which are the superpartner of the charged lepton sector, g_D does not affect our numerical results of the electron EDM and the LFV. On the other hand, real parameters g_e , β_e/α_e , γ_e/α_e in addition to complex value of τ determine the charged lepton mass matrix. By using those four real parameters g_D , g_e , β_e/α_e , γ_e/α_e and one complex parameters (Re[τ] and Im[τ]), we performed χ^2 -fit, where we adopted the sum of one-dimensional χ^2 function for four accurately known dimensionless observables, the ratio of two neutrino mass squared differences $\Delta m_{\text{atm}}^2/\Delta m_{\text{sol}}^2$, $\sin^2 \theta_{12}$, $\sin^2 \theta_{23}$ and $\sin^2 \theta_{13}$ in NuFit 5.0 [149]. In addition, we

⁴In the case of the charged lepton mass matrix with only weight 2 modular forms, a simple neutrino seesaw mass matrix is not obtained for the model of spontaneously CP violation.

⁵There are no allowed parameter set within 3σ confidence level for the inverted hierarchy of neutrino masses.

employed Gaussian approximations for fitting the charged lepton mass ratios, m_e/m_τ and m_μ/m_τ . Since free six parameters fit six observables, we can predict the CP violating Dirac phase δ_{CP}^ℓ and the sum of neutrino masses $\sum m_i$.

Parameters of the case E are shown in Appendix E.

We fix the charged lepton mass matrices by using β_e/α_e , γ_e/α_e and g_e in addition to the modulus τ in Table 3 apart from the normalization of the mass matrix. Then, the mass insertion parameters are determined including CP phases if the SUSY parameters $m_{3/2} = m_0$, $M_{1/2}$ and F^τ are put. In order to calculate the electron EDM and the branching ratio of $\mu \rightarrow e\gamma$, the slepton mass matrices of Eqs. (46) and (53) are rotated into the physical basis where the charged lepton mass matrix is real diagonal and positive.

As discussed in Eqs. (24) and (41), the magnitude of F^τ should be significantly constrained for the larger weight k_i to prevent the tachyonic slepton. Since the largest weight is $k_\tau = 7$, we take $|F^\tau| = m_0/2$ in the following numerical analyses. We will discuss later if $|F^\tau|$ is set to be larger than $= m_0/2$ with keeping the slepton mass of $\mathcal{O}(1)$ TeV.

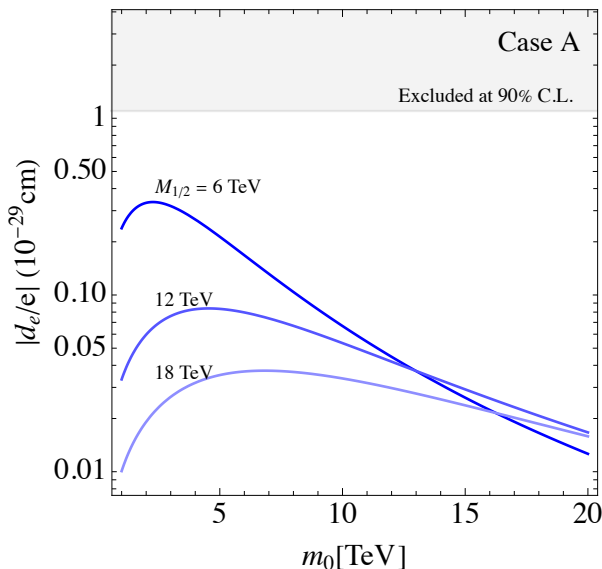


Figure 1: The predicted $|d_e/e|$ versus m_0 with putting $F^\tau = m_0/2$ in case A. The grey region is excluded by the experimental upper bound.

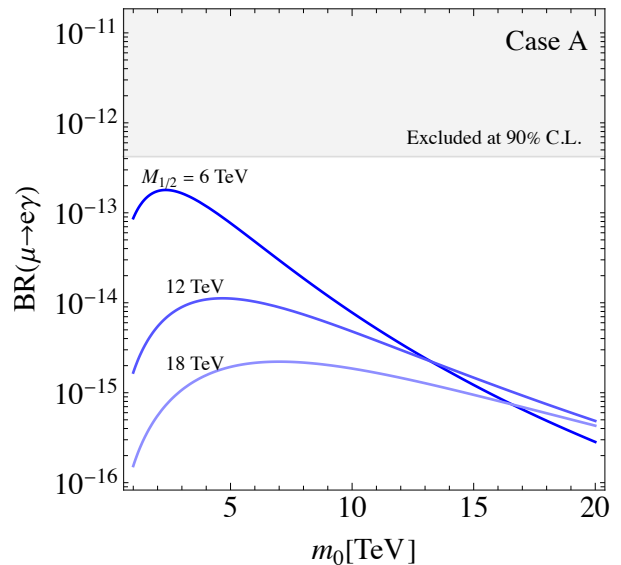


Figure 2: The predicted $\text{BR}(\mu \rightarrow e\gamma)$ versus m_0 with putting $F^\tau = m_0/2$ in case A. The grey region is excluded by the experimental upper bound.

At first, we present our numerical results of the electron EDM, $|d_e/e|$ for case A. The SUSY mass parameters are variable in $M_{1/2} = 6\text{--}18$ TeV and $m_0 = 1\text{--}20$ TeV, which are allowed in the slepton, bino and wino searches of the LHC experiments [147, 148]. We plot $|d_e/e|$ versus m_0 in Fig. 1, where $F^\tau = m_0/2$ is put. Three curved lines correspond to $M_{1/2} = 6, 12, 18$ TeV, respectively. As seen in Fig. 1, the predicted electron EDM is lower than the experimental upper bound as far as the SUSY mass scale is larger than a few TeV for $F^\tau = m_0/2$. Indeed, the predicted value is consistent with the experimental upper bound if the gaugino mass scale $M_{1/2}$ is larger than 4 TeV.

It would be helpful to comment on the behavior of the predicted curves. The maximum values are apparently found at the low m_0 region. The predicted values increase at m_0 close to 1 TeV. This behavior is due to taking $F^\tau = m_0/2$ in order to reduce the number of free parameters, although

\tilde{m}_{eRL}^2 (A -term) is proportional to F^τ and independent m_0 as seen in Eq. (46). If F^τ is fixed to, for example, 1 TeV, the prediction becomes a monotonically decreasing function against m_0 .

The SUSY mass scale is also significantly constrained by the experimental upper bound of the branching ratio for the $\mu \rightarrow e\gamma$ decay [74]. We plot $\text{BR}(\mu \rightarrow e\gamma)$ versus m_0 in Fig. 2, where we put $F^\tau = m_0/2$ again. It is found that the predicted $\text{BR}(\mu \rightarrow e\gamma)$ is lower than the experimental upper bound as far as the gaugino mass scale $M_{1/2}$ is larger than 6 TeV. Thus, the $\mu \rightarrow e\gamma$ process constrains more severely the SUSY mass scale compared with the electron EDM for case A.

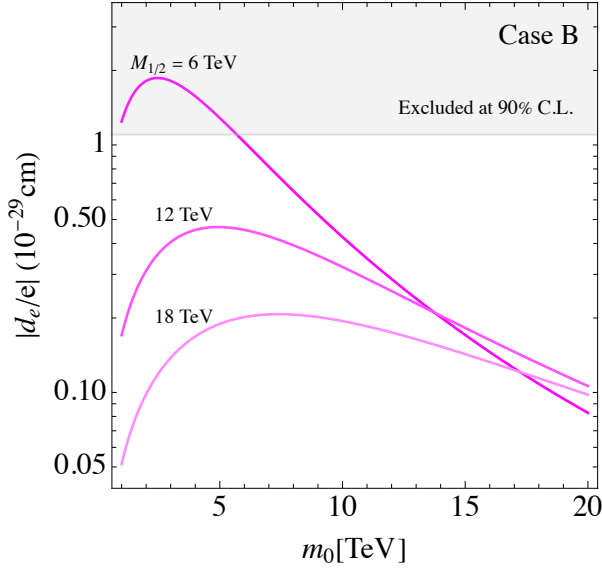


Figure 3: The predicted $|d_e/e|$ versus m_0 with putting $F^\tau = m_0/2$ in case B. The grey region is excluded by the experimental upper bound.

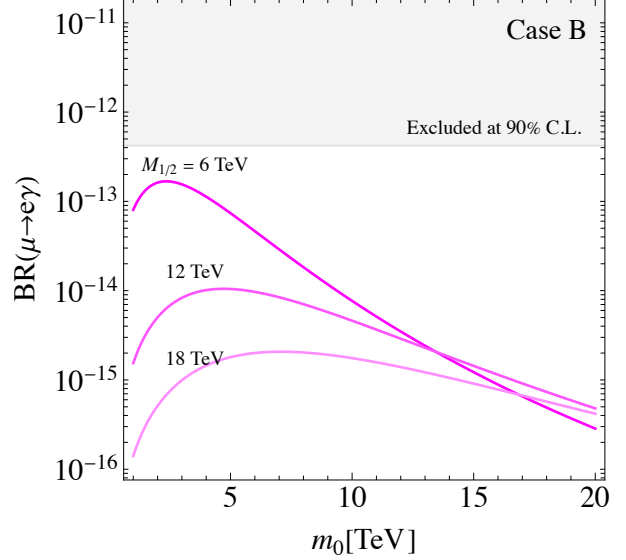


Figure 4: The predicted $\text{BR}(\mu \rightarrow e\gamma)$ versus m_0 with putting $F^\tau = m_0/2$ in case B. The grey region is excluded by the experimental upper bound.

In contrast to case A, the electron EDM constrains tightly the SUSY mass scale in case B. We present our numerical results of the electron EDM, $|d_e/e|$ and $\text{BR}(\mu \rightarrow e\gamma)$ for case B. We plot $|d_e/e|$ versus m_0 in Fig. 3, where $F^\tau = m_0/2$ is put. It is found that the predicted electron EDM exceeds the experimental upper bound at $m_0 \leq 5$ TeV if the gaugino mass scale $M_{1/2}$ is 6 TeV.

We show $\text{BR}(\mu \rightarrow e\gamma)$ versus m_0 with putting $F^\tau = m_0/2$ in Fig. 4. The predicted $\text{BR}(\mu \rightarrow e\gamma)$ is almost same as the one in case A of Fig. 2.

Thus, the constraints of the SUSY mass scale from the upper bounds $|d_e/e|$ and $\text{BR}(\mu \rightarrow e\gamma)$ depend on the model of the charged leptons.

In order to see the importance of CP phases via the modulus τ , we examine the correlation between the electron EDM and the decay rate of the $\mu \rightarrow e\gamma$ decay for both cases A and B. The correlation is clearly seen in Figs. 5 and 6. We plot them in the range of $m_0 = 1$ –20 TeV with fixing $M_{1/2} = 6$ and 18 TeV in Fig. 5, on the other hand, in the range of $M_{1/2} = 6$ –18 TeV with fixing $m_0 = 1, 10$ and 20 TeV in Fig. 6.

We find the linear correspondence between $\text{BR}(\mu \rightarrow e\gamma)$ and $|d_e/e|$ in the logarithmic coordinates for both cases A and B. The branching ratio is approximately proportional to the square of $|d_e/e|$. The slope of the line is independent of the value of F^τ , although $F^\tau = m_0/2$ is taken in these figures. Similar correlations are also found in other cases B–E. This provides a crucial test for our predictions

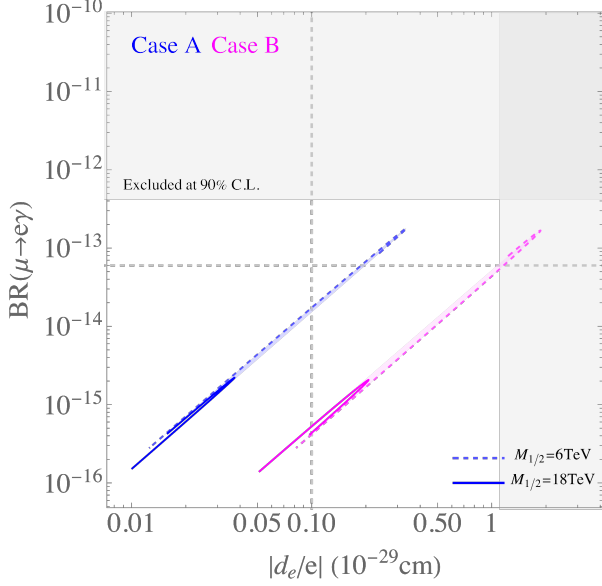


Figure 5: Plot of $|d_e/e|$ and $\text{BR}(\mu \rightarrow e\gamma)$ for cases A and B with $F^\tau = m_0/2$, where $m_0 = 1$ –20 TeV for fixed $M_{1/2} = 6$ and 18 TeV. The blue curves denotes the predictions at fixed gaugino mass $M_{1/2}$ for case A, and the pink one for case B. The grey regions are excluded by the experimental upper bounds, and the vertical and horizontal dashed grey lines indicate the future sensitivity.

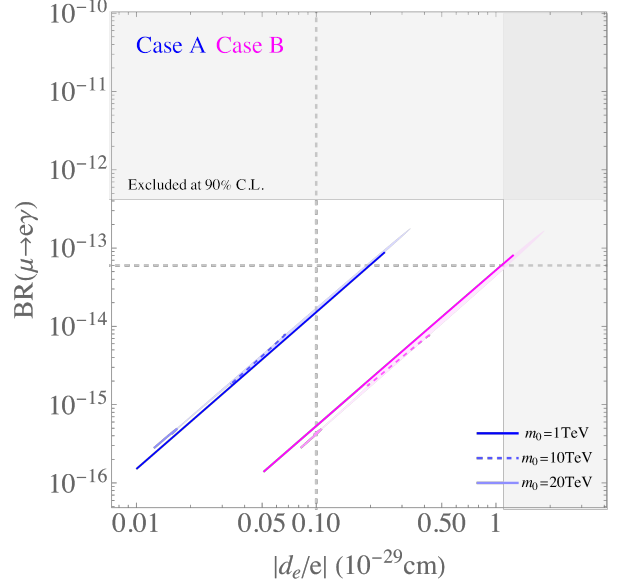


Figure 6: Plot of $|d_e/e|$ and $\text{BR}(\mu \rightarrow e\gamma)$ for cases A and B with $F^\tau = m_0/2$, where $M_{1/2} = 6$ –18 TeV for fixed $m_0 = 1, 10$ and 20 TeV. The blue curves denotes the predictions at fixed m_0 for case A, and the pink one for case B. The grey regions are excluded by the experimental upper bounds, and the vertical and horizontal dashed grey lines indicate the future sensitivity.

in future. It is also seen that the predicted decay rate of $\mu \rightarrow e\gamma$ is almost same for both cases A and B while the predicted $|d_e/e|$ of case B is larger than the one of case A in factor 5. Thus, the magnitude of the predicted electron EDM depends on the charged lepton mass matrix considerably.

Although the bound of the electron EDM is $|d_e/e| \leq 1.1 \times 10^{-29} \text{ cm}$ [116], the future sensitivity is expected to reach up to $|d_e/e| \simeq 10^{-30} \text{ cm}$ [117, 118], which is denoted by the vertical dashed grey line. For case A, their sensitive mass scale is much below 10 TeV for m_0 and $M_{1/2}$ as seen in Figs. 5 and 6. On the other hand, for case B, the electron EDM can probe the mass scale m_0 of 10–20 TeV as seen in Figs. 5 and 6. The future sensitivity of the branching ratio $\text{BR}(\mu \rightarrow e\gamma)$ is 6×10^{-14} [152], which is shown by the horizontal dashed grey line, excludes only the SUSY mass region much below 10 TeV.

Let us discuss the model dependence among A–E. We show the correlations between $|d_e/e|$ and $\text{BR}(\mu \rightarrow e\gamma)$ for all cases A–E in Figs. 7 and 8. We plot them in the range of $m_0 = 1$ –20 TeV with fixing $M_{1/2} = 6$ and 18 TeV in Fig. 7, on the other hand, in the range of $M_{1/2} = 6$ –18 TeV with fixing $m_0 = 1, 10$ and 20 TeV in Fig. 8. The predicted $|d_e/e|$ and $\text{BR}(\mu \rightarrow e\gamma)$ of case A and case C are similar each other, and those of case B and case D are also similar each other as seen in Figs. 7 and 8. The prediction of case E overlaps somewhat with the one of case A, but its region of case E extends upward considerably. The $\mu \rightarrow e\gamma$ process of case E constrains most severely the SUSY mass scale among A–E. On the other hand, the electron EDM of case D constrains most severely the SUSY mass scale.

The future sensitivity of the electron EDM, $|d_e/e| \simeq 10^{-30} \text{ cm}$ [117, 118] will probe the SUSY

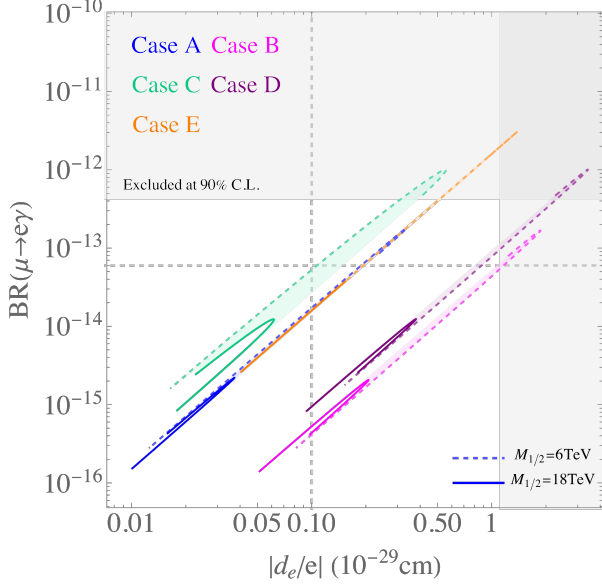


Figure 7: Plot of $|d_e/e|$ and $\text{BR}(\mu \rightarrow e\gamma)$ for all cases with $F^\tau = m_0/2$, where $m_0 = 1\text{--}20$ TeV for fixed $M_{1/2} = 6$ and 18 TeV. The blue curves denotes the predictions at fixed gaugino mass $M_{1/2}$ for case A, and the same for other cases. The grey regions are excluded by the experimental upper bounds, and the vertical and horizontal dashed grey lines indicate the future sensitivity.

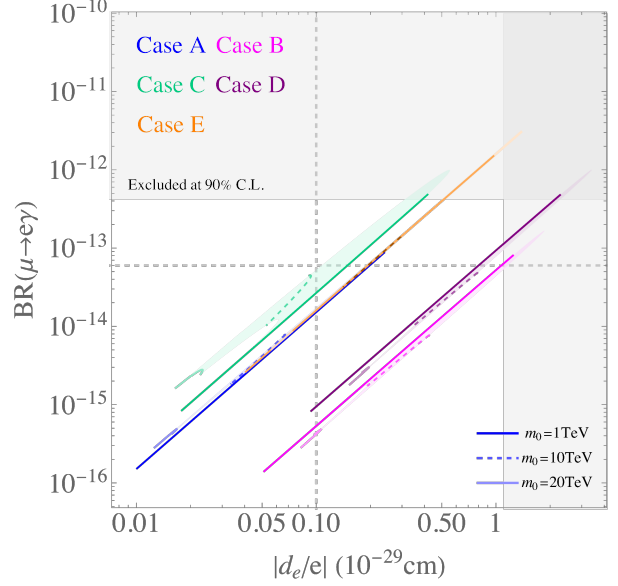


Figure 8: Plot of $|d_e/e|$ and $\text{BR}(\mu \rightarrow e\gamma)$ for all cases with $F^\tau = m_0/2$, where $M_{1/2} = 6\text{--}18$ TeV for fixed $m_0 = 1, 10$ and 20 TeV. The blue curves denotes the predictions at fixed m_0 for case A, and the same for other cases. The grey regions are excluded by the experimental upper bounds, and the vertical and horizontal dashed grey lines indicate the future sensitivity.

mass scale of $10\text{--}20$ TeV for B, D and E. On the other hand, the future sensitivity of the branching ratio $\text{BR}(\mu \rightarrow e\gamma)$, 6×10^{-14} [152] can probe the SUSY mass scale close to 10 TeV only for case E. For cases A–D, their sensitive mass scale is much below 10 TeV.

It is noted that the branching ratio of $\mu \rightarrow 3e$ and the conversion rate of $\mu N \rightarrow eN$ will be sensitive for proving the SUSY mass scale of higher than 10 TeV although the predicted branching ratio and conversion rate are significantly below the current experimental upper bounds as discussed later [153–155].

We have listed predicted mass insertion parameters and d_e/e , $\text{BR}(\mu \rightarrow e\gamma)$, $\text{BR}(\mu \rightarrow ee\bar{e})$ and $\text{CR}(\mu N \rightarrow eN)$ at $M_{1/2} = 6$ TeV, $m_0 = 10$ TeV and $F^\tau = 5$ TeV in Table 4. In this setup, the gaugino masses are given as $M_1 = 2.9$ TeV and $M_2 = 5.2$ TeV at $Q = 1$ TeV, respectively.

The dominant contribution to the electron EDM comes from the imaginary part of the single chirality flipping diagonal mass insertion $(\delta_{eLR})_{11}$ (flavor-conserving EDM) as seen in Eq. (57). Therefore, the flavor-conserving EDM is almost proportional to $\text{Im}(\delta_{eLR})_{11}$ up to its sign. The small differences of \tilde{m}_{eR} among five cases cause the slight dispersion of the proportionality. The largest flavor-conserving EDM is obtained in case D. The next-to-leading term is the flavored EDM, which arises mainly from the non-vanishing $(\delta_{eRR})_{ij}$. Therefore, it is considerably suppressed in case E since $(\delta_{eRR})_{ij}$ vanish. The largest magnitude of the flavored EDM is obtained in case C. The sum of flavor-conserving EDM and flavored one is in the range of $(0.62\text{--}7.2) \times 10^{-30}$ cm for all cases. The future experiment can reach up to this range.

We can also calculate the leading contribution of the muon EDM by using $(\delta_{eLR})_{22}$ of Table. 4.

Cases	A	B	C	D	E
$(\delta_{eLR})_{11} \times 10^8$	$0.46 - 0.56 i$	$1.8 + 3.0 i$	$-12 - 1.0 i$	$-28 - 5.6 i$	$-56 - 2.2 i$
$(\delta_{eLR})_{22} \times 10^5$	$-1.74 + 0.42 i$	$1.0 + 0.42 i$	$-1.3 - 0.39 i$	$0.62 - 0.37 i$	$-0.15 - 0.95 i$
$(\delta_{eLR})_{12} \times 10^6$	$0.91 - 4.42 i$	$-0.83 - 4.2 i$	$11 - 0.60 i$	$-11 - 1.0 i$	$7.4 + 18 i$
$(\delta_{eLR})_{13} \times 10^4$	$0.46 + 0.54 i$	$-0.45 + 0.55 i$	$1.5 + 4.3 i$	$1.4 - 3.8 i$	$0.15 - 1.9 i$
$(\delta_{eLR})_{21} \times 10^7$	$-0.21 + 0.04 i$	$-1.7 - 0.12 i$	$0.70 - 0.13 i$	$1.0 + 0.2 i$	$0.28 - 0.87 i$
$(\delta_{eLR})_{23} \times 10^5$	$0.65 - 18 i$	$-0.53 - 17 i$	$-12 - 30 i$	$-11 + 27 i$	$34.3 + 2.4 i$
$(\delta_{eLR})_{31} \times 10^7$	$-0.22 + 0.14 i$	$-0.10 + 0.49 i$	$0.62 - 0.97 i$	$-0.10 + 1.8 i$	$0.087 + 0.54 i$
$(\delta_{eRR})_{21} \times 10^5$	$-0.04 - 0.23 i$	$-48 + 21 i$	$0.19 - 0.009 i$	$26 + 1.4 i$	0
$(\delta_{eRR})_{31} \times 10^5$	$-2.99 + 2.41 i$	$-0.82 + 9.2 i$	$2.2 - 9.2 i$	$4.5 + 14 i$	0
$(\delta_{eRR})_{32} \times 10^2$	$0.72 + 1.3 i$	$0.7 - 1.2 i$	$-0.38 + 1.2 i$	$0.39 + 1.3 i$	0
flavor-conserving d_e/e cm	7.2×10^{-31}	-3.7×10^{-30}	1.3×10^{-30}	7.6×10^{-30}	2.9×10^{-30}
flavored d_e/e cm	-5.1×10^{-32}	-2.4×10^{-31}	-3.9×10^{-31}	2.5×10^{-31}	-1.9×10^{-37}
$ \sum d_e/e $ cm	6.7×10^{-31}	3.9×10^{-30}	9.1×10^{-31}	7.9×10^{-30}	2.9×10^{-30}
$\text{BR}(\mu \rightarrow e\gamma)$	7.8×10^{-15}	6.6×10^{-15}	4.5×10^{-14}	4.8×10^{-14}	1.4×10^{-13}
$\text{BR}(\mu \rightarrow ee\bar{e})$	4.6×10^{-17}	3.9×10^{-17}	2.7×10^{-16}	2.8×10^{-16}	8.3×10^{-16}
$\text{CR}(\mu N \rightarrow eN)$	5.7×10^{-17}	4.8×10^{-17}	3.3×10^{-16}	3.5×10^{-16}	1.0×10^{-15}

Table 4: Mass insertion parameters and predicted d_e/e (flavor-conserving EDM, flavored one and those sum), $\text{BR}(\mu \rightarrow e\gamma)$, $\text{BR}(\mu \rightarrow ee\bar{e})$ and $\text{CR}(\mu N \rightarrow eN)$ at $M_{1/2} = 6$ TeV, $m_0 = 10$ TeV and $F^\tau = 5$ TeV.

It is predicted as:

$$|d_\mu/e| \simeq 5 \times 10^{-27} \text{ cm}, \quad (60)$$

for case A. This predicted value is significantly below its observed upper bound, 2×10^{-19} at BNL-E821 [118]. The improvement up to 2×10^{-21} is expected at FNAL [118].

The leading terms of the branching ratio $\text{BR}(\mu \rightarrow e\gamma)$ are given in terms of $(\delta_{eLR})_{12}$ and $(\delta_{eLR})_{12}^*$ as seen in Eq. (58) due to the chiral enhancement. The next-to-leading ones arise from $(\delta_{eRR})_{ij}$. However, the contribution of the next-to-leading terms are suppressed enough compared with the leading ones in all cases. The branching ratio is predicted in rather broad range $6.6 \times 10^{-15} - 9.4 \times 10^{-14}$ for all cases. Case E will be tested since the future sensitivity is expected to be 6×10^{-14} [152].

In SUSY models, the branching ratio of $\mu \rightarrow 3e$ and the conversion rate of $\mu N \rightarrow eN$ are simply related to $\text{BR}(\mu \rightarrow e\gamma)$ as seen in Eq. (59). The five branching ratio and conversion rate are enough below the current experimental upper bounds 1.0×10^{-12} and 7.0×10^{-13} [157], respectively, as seen in Table 4. Since future experiments will explore these predictions at the level of 10^{-16} for $\mu \rightarrow 3e$ and $\mu N \rightarrow eN$ [153–155], it will probe the SUSY mass scale of $m_0 \simeq 10$ TeV.

We can also calculate the branching ratios of tauon decays, $\tau \rightarrow e\gamma$ and $\tau \rightarrow \mu\gamma$. Both branching ratios are at most $\mathcal{O}(10^{-13})$, which are much below the current experimental upper bounds 3.3×10^{-8} and 4.4×10^{-8} , respectively [157].

As well known, large flavor-violating trilinear coupling may generate instabilities of the electroweak vacuum, which constrains the magnitudes of mass insertion parameters δ_{eLR} [156]. It is noted that our predicted ones do not spoil the vacuum stability.

We also comment on the effect of neutrino Yukawa matrix in the type-I seesaw to the $\mu \rightarrow e\gamma$ decay. If there are right-handed neutrinos which couple to the left-handed neutrinos via Yukawa couplings, the RGEs effects, which is the running from the high scale Q_0 to the right-handed Majorana mass scale M_R , can also induce off-diagonal elements in the slepton mass matrix as follows [158, 159]:

$$(\delta_{eLL})_{12} \simeq -\frac{6m_0^2}{16\pi^2 m_{\text{slepton}}^2} (Y_D^\dagger Y_D)_{12} \ln \frac{Q_0}{M_R}, \quad (61)$$

where Y_D is Dirac neutrino Yukawa matrix in the diagonal base of the charged lepton. One should check its effect to the $\mu \rightarrow e\gamma$ decay since our models use type-I seesaw. In conclusion, the effect of neutrino Yukawa couplings is still at the next-to-leading order of our prediction as far as we take $M_R \leq 10^{13}$ GeV. For example, in case A, we have

$$(\delta_{eLL})_{12} \simeq 4.9 \times 10^{-3} \ (6.6 \times 10^{-4}), \quad \text{BR}(\mu \rightarrow e\gamma) \simeq 4.8 \times 10^{-16} \ (8.5 \times 10^{-18}), \quad (62)$$

for $M_R = 10^{13} \ (10^{12})$ GeV, where we take $M_1 = 2.9$ TeV, $M_2 = 5.2$ TeV and $m_{\text{slepton}} = m_0 = 10$ TeV, and the branching ratio includes only the contribution of neutrino Yukawa couplings.

In our numerical results, we take $F^\tau = m_0/2$ to prevent the tachyonic slepton since the largest weight is $k_\tau = 7$ in our lepton mass matrix. Our predicted electron EDM is almost proportional to the magnitude of F^τ , and the branching ratio of $\mu \rightarrow e\gamma$ is roughly proportional to $|F^\tau|^2$ in the following numerical analyses. We have checked the numerical results in the case of $F^\tau = m_0$ for case E, where tachyonic sleptons are prevented due to small weight 1. Indeed, the calculated $|d_e/e|$ is approximately two times larger than the one for $F^\tau = m_0/2$, while $\text{BR}(\mu \rightarrow e\gamma)$ is four times larger. Thus, we can estimate roughly $|F^\tau|$ dependence of our numerical results.

7 Summary

We have studied the electron EDM in the supersymmetric A_4 modular invariant theory of flavors with CP invariance. The CP symmetry of the lepton sector is broken by fixing modulus τ . In this framework, a fixed τ also causes the CP violation in the soft SUSY breaking terms. The electron EDM arises from this CP non-conserved soft SUSY breaking terms. We have examined the electron EDM in the five cases A–E of charged lepton mass matrices, which are completely consistent with observed lepton masses and PMNS mixing angles. It is found that the present upper bound of $|d_e/e| \leq 1.1 \times 10^{-29}$ excludes the SUSY mass scale, m_0 and $M_{1/2}$ below 4–6 TeV depending on cases A–E.

The SUSY mass scale is also significantly constrained by considering the experimental upper bound of the branching ratio of the $\mu \rightarrow e\gamma$ decay.

In order to see the effect of CP phase in the modulus τ , we examine the correlation between the electron EDM and the decay rate of the $\mu \rightarrow e\gamma$ decay. The correlations are clearly seen in contrast to models of the conventional flavor symmetry. We have found the linear correspondence $\text{BR}(\mu \rightarrow e\gamma)$ between $|d_e/e|$ in the logarithmic coordinates for cases A–E. The branching ratio is approximately proportional to the square of $|d_e/e|$. The slope of the line is independent of the value of F^τ although $F^\tau = m_0/2$ is taken in our calculations.

The predicted d_e/e and $\text{BR}(\mu \rightarrow e\gamma)$ of case A and case C are similar each other, and those of case B and case D are also similar each other. The $\mu \rightarrow e\gamma$ decay constrains most severely the SUSY

mass scale in case E compared with other cases. On the other hand, the electron EDM constrains most severely the SUSY mass scale in case D among five cases.

Although the current experimental upper bound of the electron EDM is $|d_e/e| \leq 1.1 \times 10^{-29} \text{ cm}$, the future sensitivity of the electron EDM is expected to reach up to $|d_e/e| \simeq 10^{-30} \text{ cm}$. Then, the SUSY mass scale will be significantly constrained by $|d_e/e|$. Indeed, it will probe the SUSY mass scale of 10–20 TeV.

On the other hand, the future sensitivity of the branching ratio $\text{BR}(\mu \rightarrow e\gamma)$, 6×10^{-14} probes at most the SUSY mass scale of 10 TeV. It is also remarked that the branching ratio of $\mu \rightarrow 3e$ and the conversion rate of $\mu N \rightarrow eN$ will be sensitive for probing the SUSY mass scale of higher than 10 TeV.

Thus, the electron EDM provides a severe test of the CP violation via the modulus τ in the supersymmetric modular invariant theory of flavors.

Acknowledgments

We thank Tatsuo Kobayashi for useful discussions. The work of K.Y. was supported by the JSPS KAKENHI 21K13923.

Appendix

A Tensor product of A_4 group

We take the generators of A_4 group for the triplet as follows:

$$S = \frac{1}{3} \begin{pmatrix} -1 & 2 & 2 \\ 2 & -1 & 2 \\ 2 & 2 & -1 \end{pmatrix}, \quad T = \begin{pmatrix} 1 & 0 & 0 \\ 0 & \omega & 0 \\ 0 & 0 & \omega^2 \end{pmatrix}, \quad (63)$$

where $\omega = e^{i\frac{2}{3}\pi}$ for a triplet. In this base, the multiplication rule is

$$\begin{aligned} \begin{pmatrix} a_1 \\ a_2 \\ a_3 \end{pmatrix}_{\mathbf{3}} \otimes \begin{pmatrix} b_1 \\ b_2 \\ b_3 \end{pmatrix}_{\mathbf{3}} &= (a_1b_1 + a_2b_3 + a_3b_2)_{\mathbf{1}} \oplus (a_3b_3 + a_1b_2 + a_2b_1)_{\mathbf{1}'} \\ &\quad \oplus (a_2b_2 + a_1b_3 + a_3b_1)_{\mathbf{1}''} \\ &\quad \oplus \frac{1}{3} \begin{pmatrix} 2a_1b_1 - a_2b_3 - a_3b_2 \\ 2a_3b_3 - a_1b_2 - a_2b_1 \\ 2a_2b_2 - a_1b_3 - a_3b_1 \end{pmatrix}_{\mathbf{3}} \oplus \frac{1}{2} \begin{pmatrix} a_2b_3 - a_3b_2 \\ a_1b_2 - a_2b_1 \\ a_3b_1 - a_1b_3 \end{pmatrix}_{\mathbf{3}}, \\ \mathbf{1} \otimes \mathbf{1} &= \mathbf{1}, \quad \mathbf{1}' \otimes \mathbf{1}' = \mathbf{1}'', \quad \mathbf{1}'' \otimes \mathbf{1}'' = \mathbf{1}', \quad \mathbf{1}' \otimes \mathbf{1}'' = \mathbf{1}, \end{aligned} \quad (64)$$

where

$$T(\mathbf{1}') = \omega, \quad T(\mathbf{1}'') = \omega^2. \quad (65)$$

More details are shown in the review [2, 3].

B Modular forms with weight 2, 4, 6, 8 in Γ_3 group

We present modular forms with weight 2, 4, 6, 8 in A_4 modular group. The triplet modular forms can be written in terms of $\eta(\tau)$ and its derivative [11]:

$$\begin{aligned} Y_1 &= \frac{i}{2\pi} \left(\frac{\eta'(\tau/3)}{\eta(\tau/3)} + \frac{\eta'((\tau+1)/3)}{\eta((\tau+1)/3)} + \frac{\eta'((\tau+2)/3)}{\eta((\tau+2)/3)} - \frac{27\eta'(3\tau)}{\eta(3\tau)} \right), \\ Y_2 &= \frac{-i}{\pi} \left(\frac{\eta'(\tau/3)}{\eta(\tau/3)} + \omega^2 \frac{\eta'((\tau+1)/3)}{\eta((\tau+1)/3)} + \omega \frac{\eta'((\tau+2)/3)}{\eta((\tau+2)/3)} \right), \\ Y_3 &= \frac{-i}{\pi} \left(\frac{\eta'(\tau/3)}{\eta(\tau/3)} + \omega \frac{\eta'((\tau+1)/3)}{\eta((\tau+1)/3)} + \omega^2 \frac{\eta'((\tau+2)/3)}{\eta((\tau+2)/3)} \right). \end{aligned} \quad (66)$$

They are also expressed in the q expansions, where $q = e^{i2\pi\tau}$, as follows:

$$\mathbf{Y}_3^{(2)}(\tau) = \begin{pmatrix} Y_1 \\ Y_2 \\ Y_3 \end{pmatrix} = \begin{pmatrix} 1 + 12q + 36q^2 + 12q^3 + \dots \\ -6q^{1/3}(1 + 7q + 8q^2 + \dots) \\ -18q^{2/3}(1 + 2q + 5q^2 + \dots) \end{pmatrix}. \quad (67)$$

For weight 4, there are five modular forms by the tensor product of $\mathbf{3} \otimes \mathbf{3}$ as:

$$\begin{aligned} \mathbf{Y}_1^{(4)}(\tau) &= Y_1^2 + 2Y_2Y_3, & \mathbf{Y}_{1'}^{(4)}(\tau) &= Y_3^2 + 2Y_1Y_2, \\ \mathbf{Y}_3^{(4)}(\tau) &= \begin{pmatrix} Y_1^{(4)} \\ Y_2^{(4)} \\ Y_3^{(4)} \end{pmatrix} = \begin{pmatrix} Y_1^2 - Y_2Y_3 \\ Y_3^2 - Y_1Y_2 \\ Y_2^2 - Y_1Y_3 \end{pmatrix}. \end{aligned} \quad (68)$$

For $k = 6$, there are seven modular forms by the tensor products of A_4 as:

$$\begin{aligned} \mathbf{Y}_1^{(6)} &= Y_1^3 + Y_2^3 + Y_3^3 - 3Y_1Y_2Y_3, \\ \mathbf{Y}_3^{(6)} &\equiv \begin{pmatrix} Y_1^{(6)} \\ Y_2^{(6)} \\ Y_3^{(6)} \end{pmatrix} = (Y_1^2 + 2Y_2Y_3) \begin{pmatrix} Y_1 \\ Y_2 \\ Y_3 \end{pmatrix}, & \mathbf{Y}_{3'}^{(6)} &\equiv \begin{pmatrix} Y_1'^{(6)} \\ Y_2'^{(6)} \\ Y_3'^{(6)} \end{pmatrix} = (Y_3^2 + 2Y_1Y_2) \begin{pmatrix} Y_3 \\ Y_1 \\ Y_2 \end{pmatrix}. \end{aligned} \quad (69)$$

For $k = 8$, there are 9 modular forms by the tensor products of A_4 as:

$$\begin{aligned} \mathbf{Y}_1^{(8)} &= (Y_1^2 + 2Y_2Y_3)^2, & \mathbf{Y}_{1'}^{(8)} &= (Y_1^2 + 2Y_2Y_3)(Y_3^2 + 2Y_1Y_2), & \mathbf{Y}_{1''}^{(8)} &= (Y_3^2 + 2Y_1Y_2)^2, \\ \mathbf{Y}_3^{(8)} &\equiv \begin{pmatrix} Y_1^{(8)} \\ Y_2^{(8)} \\ Y_3^{(8)} \end{pmatrix} = (Y_1^3 + Y_2^3 + Y_3^3 - 3Y_1Y_2Y_3) \begin{pmatrix} Y_1 \\ Y_2 \\ Y_3 \end{pmatrix}, & \mathbf{Y}_{3'}^{(8)} &\equiv \begin{pmatrix} Y_1'^{(8)} \\ Y_2'^{(8)} \\ Y_3'^{(8)} \end{pmatrix} = (Y_3^2 + 2Y_1Y_2) \begin{pmatrix} Y_2^2 - Y_1Y_3 \\ Y_1^2 - Y_2Y_3 \\ Y_3^2 - Y_1Y_2 \end{pmatrix}. \end{aligned}$$

C RGEs of leptons and slepton

The relevant RGEs are given by [141, 142];

$$\begin{aligned}
16\pi^2 \frac{d}{dt} (\tilde{m}_{eL}^2)_{ij} &= - \left(\frac{6}{5} g_1^2 |M_1|^2 + 6g_2^2 |M_2|^2 \right) \delta_{ij} - \frac{3}{5} g_1^2 S \delta_{ij} \\
&\quad + ((\tilde{m}_{eL}^2) Y_e^\dagger Y_e + Y_e^\dagger Y_e (\tilde{m}_{eL}^2)_K)_{ij} \\
&\quad + 2 (Y_e^\dagger (\tilde{m}_{eR}^2)_K Y_e + \tilde{m}_{H_d}^2 Y_e^\dagger Y_e + A_e^\dagger A_e)_{ij} , \\
16\pi^2 \frac{d}{dt} (\tilde{m}_{eR}^2)_{ij} &= - \frac{24}{5} g_1^2 |M_1|^2 \delta_{ij} + \frac{6}{5} g_1^2 S \delta_{ij} \\
&\quad + 2 ((\tilde{m}_{eR}^2)_K Y_e Y_e^\dagger + Y_e Y_e^\dagger (\tilde{m}_{eR}^2)_K)_{ij} \\
&\quad + 4 (Y_e (\tilde{m}_{eL}^2)_K Y_e^\dagger + m_{H_d}^2 Y_e Y_e^\dagger + A_e A_e^\dagger)_{ij} , \\
16\pi^2 \frac{d}{dt} (A_e)_{ij} &= \left(-\frac{9}{5} g_1^2 - 3g_2^2 + 3\text{Tr}(Y_d^\dagger Y_d) + \text{Tr}(Y_e^\dagger Y_e) \right) (A_e)_{ij} \\
&\quad + 2 \left(\frac{9}{5} g_1^2 M_1 + 3g_2^2 M_2 + 3\text{Tr}(Y_d^\dagger A_d) + \text{Tr}(Y_e^\dagger A_e) \right) Y_{eij} \\
&\quad + 4 (Y_e Y_e^\dagger A_e)_{ij} + 5 (A_e Y_e^\dagger Y_e)_{ij} , \\
16\pi^2 \frac{d}{dt} Y_{eij} &= \left(-\frac{9}{5} g_1^2 - 3g_2^2 + 3\text{Tr}(Y_d Y_d^\dagger) + \text{Tr}(Y_e Y_e^\dagger) \right) Y_{eij} + 3 (Y_e Y_e^\dagger Y_e)_{ij} .
\end{aligned} \tag{70}$$

In these expressions, $g_{1,2}$ are the gauge couplings of $\text{SU}(2)_L \times U(1)_Y$, $M_{1,2}$ are the corresponding gaugino mass terms, $Y_{e,d}$ are the Yukawa couplings for charged leptons and down quarks, $A_e = (\tilde{m}_{eLR}^2)/v_d$, and

$$S = \text{Tr}(\tilde{m}_{qL}^2 + \tilde{m}_{dR}^2 - 2\tilde{m}_{uR}^2 - \tilde{m}_{eL}^2 + \tilde{m}_{eR}^2) - \tilde{m}_{H_d}^2 + \tilde{m}_{H_u}^2 ,$$

where \tilde{m}_{qL}^2 , \tilde{m}_{dL}^2 , \tilde{m}_{uR}^2 are mass matrices of squarks and \tilde{m}_{H_u} and \tilde{m}_{H_d} are the Higgs masses. The parameter t is $t = \ln Q/Q_0$, where Q is the renormalization scale and Q_0 is a reference scale.

D Loop functions

The dimensionless functions C_B , $C'_{B,R}$, $C'_{B,L}$ and C''_B are given approximately as [102]:

$$C_B \simeq h_1(\bar{x}) , \tag{71}$$

$$C'_{B,R} \simeq C'_{B,L} \simeq \frac{1}{2} [h_1(\bar{x}) + k_1(\bar{x})] , \tag{72}$$

$$C''_B \simeq \frac{1}{3} [h_1(\bar{x}) + 2k_1(\bar{x})] , \tag{73}$$

$$\tag{74}$$

where we take $\tilde{m}_e = \sqrt{\tilde{m}_{eL} \tilde{m}_{eR}}$ as the average slepton mass and put $\bar{x} = (M_1/\tilde{m}_e)^2$.

On the other hand, functions C'_L , C'_R and C'_2 are exactly given as:

$$C'_L = C_0 \frac{1}{m_{eL}^2} \frac{y_L}{y_L - x_L} [h_1(x_L) - h_1(y_L)], \quad (75)$$

$$C'_R = C_0 \frac{1}{m_{eR}^2} \frac{y_R}{y_R - x_R} [h_1(x_R) - h_1(y_R)], \quad (76)$$

$$C'_2 = C_0 \frac{M_2 \cot^2 \theta_W}{M_1 m_{eL}^2} \frac{y_L}{y_L - x'_L} [h_2(x'_L) - h_2(y_L)], \quad (77)$$

$$(78)$$

with

$$x_L = \frac{M_1^2}{m_{eL}^2}, \quad x_R = \frac{M_1^2}{m_{eR}^2}, \quad x'_L = \frac{M_2^2}{m_{eL}^2}, \quad y_L = \frac{\mu^2}{m_{eL}^2}, \quad y_R = \frac{\mu^2}{m_{eR}^2}, \quad (79)$$

where $C_0 = m_0^4/\mu^2$. Functions $h_1(x)$, $h_2(x)$ and $k_1(x)$ are defined as:

$$h_1(x) = \frac{1 + 4x - 5x^2 + (2x^2 + 4x) \ln x}{(1 - x)^4}, \quad (80)$$

$$h_2(x) = \frac{7x^2 + 4x - 11 - 2(x^2 + 6x + 2) \ln x}{2(x - 1)^4}, \quad (81)$$

$$k_1(x) = \frac{d}{dx} [x h_1(x)]. \quad (82)$$

Note that M_i and μ^2 are real positive values.

E Mass matrix M_e with only weight 2 modular forms

We present the charged lepton mass matrix in terms of only weight 2 modular forms, in which $\text{BR}(\mu \rightarrow e\gamma)$ was discussed in Ref. [74]. The mass matrix is given as:

$$M_e = v_d \begin{pmatrix} \alpha_e & 0 & 0 \\ 0 & \beta_e & 0 \\ 0 & 0 & \gamma_e \end{pmatrix} \begin{pmatrix} Y_1 & Y_3 & Y_2 \\ Y_2 & Y_1 & Y_3 \\ Y_3 & Y_2 & Y_1 \end{pmatrix}, \quad (83)$$

where Y_i 's are given in Eq. (66). The neutrino mass matrix is given by the dimension five Weinberg operator. We present the best fit parameter set for the observed lepton masses and flavor mixing angles [68] as follows:

$$E : \quad \tau = -0.0796 + 1.0065i, \quad \alpha_e/\gamma_e = 6.82 \times 10^{-2}, \quad \beta_e/\gamma_e = 1.02 \times 10^{-3}, \quad (84)$$

which is referred as the case E in the text.

The slepton mass matrix \tilde{m}_{eRL}^2 including RGE effect is written as:

$$\tilde{m}_{eRL}^2 \simeq 1.4 v_d \left[-m_F \begin{pmatrix} \alpha_e & 0 & 0 \\ 0 & \beta_e & 0 \\ 0 & 0 & \gamma_e \end{pmatrix} \begin{pmatrix} Y_1 & Y_3 & Y_2 \\ Y_2 & Y_1 & Y_3 \\ Y_3 & Y_2 & Y_1 \end{pmatrix} + F^\tau \begin{pmatrix} \alpha_e & 0 & 0 \\ 0 & \beta_e & 0 \\ 0 & 0 & \gamma_e \end{pmatrix} \frac{d}{d\tau} \begin{pmatrix} Y_1 & Y_3 & Y_2 \\ Y_2 & Y_1 & Y_3 \\ Y_3 & Y_2 & Y_1 \end{pmatrix} \right]. \quad (85)$$

Since the first term of the right-hand side is proportional to M_e , it does not contribute to $|d_e/e|$ and $\text{BR}(\mu \rightarrow e\gamma)$. On the other hand, \tilde{m}_{eLL}^2 and \tilde{m}_{eRR}^2 are proportional to the unit matrix. Then, these mass terms do not contribute to $|d_e/e|$ and $\text{BR}(\mu \rightarrow e\gamma)$.

References

- [1] G. Altarelli and F. Feruglio, *Rev. Mod. Phys.* **82** (2010) 2701 [arXiv:1002.0211 [hep-ph]].
- [2] H. Ishimori, T. Kobayashi, H. Ohki, Y. Shimizu, H. Okada and M. Tanimoto, *Prog. Theor. Phys. Suppl.* **183** (2010) 1 [arXiv:1003.3552 [hep-th]].
- [3] H. Ishimori, T. Kobayashi, H. Ohki, H. Okada, Y. Shimizu and M. Tanimoto, *Lect. Notes Phys.* **858** (2012) 1, Springer.
- [4] D. Hernandez and A. Y. Smirnov, *Phys. Rev. D* **86** (2012) 053014 [arXiv:1204.0445 [hep-ph]].
- [5] S. F. King and C. Luhn, *Rept. Prog. Phys.* **76** (2013) 056201 [arXiv:1301.1340 [hep-ph]].
- [6] S. F. King, A. Merle, S. Morisi, Y. Shimizu and M. Tanimoto, *New J. Phys.* **16**, 045018 (2014) [arXiv:1402.4271 [hep-ph]].
- [7] M. Tanimoto, *AIP Conf. Proc.* **1666** (2015) 120002.
- [8] S. F. King, *Prog. Part. Nucl. Phys.* **94** (2017) 217 [arXiv:1701.04413 [hep-ph]].
- [9] S. T. Petcov, *Eur. Phys. J. C* **78** (2018) no.9, 709 [arXiv:1711.10806 [hep-ph]].
- [10] F. Feruglio and A. Romanino, arXiv:1912.06028 [hep-ph].
- [11] F. Feruglio, in *From My Vast Repertoire ...: Guido Altarelli's Legacy*, A. Levy, S. Forte, Stefano, and G. Ridolfi, eds., pp.227–266, 2019, arXiv:1706.08749 [hep-ph].
- [12] R. de Adelhart Toorop, F. Feruglio and C. Hagedorn, *Nucl. Phys. B* **858**, 437 (2012) [arXiv:1112.1340 [hep-ph]].
- [13] T. Kobayashi, K. Tanaka and T. H. Tatsuishi, *Phys. Rev. D* **98** (2018) no.1, 016004 [arXiv:1803.10391 [hep-ph]].
- [14] J. T. Penedo and S. T. Petcov, *Nucl. Phys. B* **939** (2019) 292 [arXiv:1806.11040 [hep-ph]].
- [15] P. P. Novichkov, J. T. Penedo, S. T. Petcov and A. V. Titov, *JHEP* **1904** (2019) 174 [arXiv:1812.02158 [hep-ph]].
- [16] J. C. Criado and F. Feruglio, *SciPost Phys.* **5** (2018) no.5, 042 [arXiv:1807.01125 [hep-ph]].
- [17] T. Kobayashi, N. Omoto, Y. Shimizu, K. Takagi, M. Tanimoto and T. H. Tatsuishi, *JHEP* **1811** (2018) 196 [arXiv:1808.03012 [hep-ph]].
- [18] G. J. Ding, S. F. King and X. G. Liu, *JHEP* **1909** (2019) 074 [arXiv:1907.11714 [hep-ph]].
- [19] P. P. Novichkov, J. T. Penedo, S. T. Petcov and A. V. Titov, *JHEP* **1904** (2019) 005 [arXiv:1811.04933 [hep-ph]].
- [20] T. Kobayashi, Y. Shimizu, K. Takagi, M. Tanimoto and T. H. Tatsuishi, *JHEP* **02** (2020), 097 [arXiv:1907.09141 [hep-ph]].

- [21] X. Wang and S. Zhou, JHEP **05** (2020), 017 [arXiv:1910.09473 [hep-ph]].
- [22] G. J. Ding, S. F. King and X. G. Liu, Phys. Rev. D **100** (2019) no.11, 115005 [arXiv:1903.12588 [hep-ph]].
- [23] X. G. Liu and G. J. Ding, JHEP **1908** (2019) 134 [arXiv:1907.01488 [hep-ph]].
- [24] P. Chen, G. J. Ding, J. N. Lu and J. W. F. Valle, Phys. Rev. D **102** (2020) no.9, 095014 [arXiv:2003.02734 [hep-ph]].
- [25] P. P. Novichkov, J. T. Penedo and S. T. Petcov, Nucl. Phys. B **963** (2021), 115301 [arXiv:2006.03058 [hep-ph]].
- [26] X. G. Liu, C. Y. Yao and G. J. Ding, Phys. Rev. D **103** (2021) no.5, 056013 [arXiv:2006.10722 [hep-ph]].
- [27] I. de Medeiros Varzielas, S. F. King and Y. L. Zhou, Phys. Rev. D **101** (2020) no.5, 055033 [arXiv:1906.02208 [hep-ph]].
- [28] G. J. Ding, S. F. King, C. C. Li and Y. L. Zhou, JHEP **08** (2020), 164 [arXiv:2004.12662 [hep-ph]].
- [29] T. Asaka, Y. Heo, T. H. Tatsuishi and T. Yoshida, JHEP **2001** (2020) 144 [arXiv:1909.06520 [hep-ph]].
- [30] T. Asaka, Y. Heo and T. Yoshida, Phys. Lett. B **811** (2020), 135956 [arXiv:2009.12120 [hep-ph]].
- [31] M. K. Behera, S. Mishra, S. Singirala and R. Mohanta, [arXiv:2007.00545 [hep-ph]].
- [32] S. Mishra, [arXiv:2008.02095 [hep-ph]].
- [33] F. J. de Anda, S. F. King and E. Perdomo, Phys. Rev. D **101** (2020) no.1, 015028 [arXiv:1812.05620 [hep-ph]].
- [34] T. Kobayashi, Y. Shimizu, K. Takagi, M. Tanimoto and T. H. Tatsuishi, arXiv:1906.10341 [hep-ph].
- [35] P. P. Novichkov, S. T. Petcov and M. Tanimoto, Phys. Lett. B **793** (2019) 247 [arXiv:1812.11289 [hep-ph]].
- [36] T. Kobayashi, Y. Shimizu, K. Takagi, M. Tanimoto, T. H. Tatsuishi and H. Uchida, Phys. Lett. B **794** (2019) 114 [arXiv:1812.11072 [hep-ph]].
- [37] H. Okada and M. Tanimoto, Phys. Lett. B **791** (2019) 54 [arXiv:1812.09677 [hep-ph]].
- [38] H. Okada and M. Tanimoto, Eur. Phys. J. C **81** (2021) no.1, 52 [arXiv:1905.13421 [hep-ph]].
- [39] T. Nomura and H. Okada, Phys. Lett. B **797** (2019) 134799 [arXiv:1904.03937 [hep-ph]].
- [40] H. Okada and Y. Orikasa, Phys. Rev. D **100** (2019) no.11, 115037 [arXiv:1907.04716 [hep-ph]].

- [41] Y. Kariyazono, T. Kobayashi, S. Takada, S. Tamba and H. Uchida, Phys. Rev. D **100** (2019) no.4, 045014 [arXiv:1904.07546 [hep-th]].
- [42] T. Nomura and H. Okada, Nucl. Phys. B **966** (2021), 115372 [arXiv:1906.03927 [hep-ph]].
- [43] H. Okada and Y. Orikasa, arXiv:1908.08409 [hep-ph].
- [44] T. Nomura, H. Okada and O. Popov, Phys. Lett. B **803** (2020) 135294 [arXiv:1908.07457 [hep-ph]].
- [45] J. C. Criado, F. Feruglio and S. J. D. King, JHEP **2002** (2020) 001 [arXiv:1908.11867 [hep-ph]].
- [46] S. F. King and Y. L. Zhou, Phys. Rev. D **101** (2020) no.1, 015001 [arXiv:1908.02770 [hep-ph]].
- [47] G. J. Ding, S. F. King, X. G. Liu and J. N. Lu, JHEP **1912** (2019) 030 [arXiv:1910.03460 [hep-ph]].
- [48] I. de Medeiros Varzielas, M. Levy and Y. L. Zhou, JHEP **11** (2020), 085 [arXiv:2008.05329 [hep-ph]].
- [49] D. Zhang, Nucl. Phys. B **952** (2020) 114935 [arXiv:1910.07869 [hep-ph]].
- [50] T. Nomura, H. Okada and S. Patra, Nucl. Phys. B **967** (2021), 115395 [arXiv:1912.00379 [hep-ph]].
- [51] T. Kobayashi, T. Nomura and T. Shimomura, Phys. Rev. D **102** (2020) no.3, 035019 [arXiv:1912.00637 [hep-ph]].
- [52] J. N. Lu, X. G. Liu and G. J. Ding, Phys. Rev. D **101** (2020) no.11, 115020 [arXiv:1912.07573 [hep-ph]].
- [53] X. Wang, Nucl. Phys. B **957** (2020), 115105 [arXiv:1912.13284 [hep-ph]].
- [54] S. J. D. King and S. F. King, JHEP **09** (2020), 043 [arXiv:2002.00969 [hep-ph]].
- [55] M. Abbas, Phys. Rev. D **103** (2021) no.5, 056016 [arXiv:2002.01929 [hep-ph]].
- [56] H. Okada and Y. Shoji, Phys. Dark Univ. **31** (2021), 100742 [arXiv:2003.11396 [hep-ph]].
- [57] H. Okada and Y. Shoji, Nucl. Phys. B **961** (2020), 115216 [arXiv:2003.13219 [hep-ph]].
- [58] G. J. Ding and F. Feruglio, JHEP **06** (2020), 134 [arXiv:2003.13448 [hep-ph]].
- [59] T. Nomura and H. Okada, [arXiv:2007.04801 [hep-ph]].
- [60] T. Nomura and H. Okada, arXiv:2007.15459 [hep-ph].
- [61] H. Okada and M. Tanimoto, [arXiv:2005.00775 [hep-ph]].
- [62] H. Okada and M. Tanimoto, Phys. Rev. D **103** (2021) no.1, 015005 [arXiv:2009.14242 [hep-ph]].
- [63] K. I. Nagao and H. Okada, JCAP **05** (2021), 063 [arXiv:2008.13686 [hep-ph]].

- [64] K. I. Nagao and H. Okada, [arXiv:2010.03348 [hep-ph]].
- [65] C. Y. Yao, X. G. Liu and G. J. Ding, Phys. Rev. D **103**, no.9, 095013 (2021) [arXiv:2011.03501 [hep-ph]].
- [66] X. Wang, B. Yu and S. Zhou, Phys. Rev. D **103** (2021) no.7, 076005 [arXiv:2010.10159 [hep-ph]].
- [67] M. Abbas, Phys. Atom. Nucl. **83** (2020) no.5, 764-769.
- [68] H. Okada and M. Tanimoto, JHEP **03** (2021), 010 [arXiv:2012.01688 [hep-ph]].
- [69] C. Y. Yao, J. N. Lu and G. J. Ding, [arXiv:2012.13390 [hep-ph]].
- [70] F. Feruglio, V. Gherardi, A. Romanino and A. Titov, JHEP **05**, 242 (2021) [arXiv:2101.08718 [hep-ph]].
- [71] S. F. King and Y. L. Zhou, JHEP **04** (2021), 291 [arXiv:2103.02633 [hep-ph]].
- [72] P. Chen, G. J. Ding and S. F. King, JHEP **04** (2021), 239 [arXiv:2101.12724 [hep-ph]].
- [73] X. Du and F. Wang, [arXiv:2012.01397 [hep-ph]].
- [74] T. Kobayashi, T. Shimomura and M. Tanimoto, [arXiv:2102.10425 [hep-ph]].
- [75] P. P. Novichkov, J. T. Penedo and S. T. Petcov, JHEP **04**, 206 (2021) [arXiv:2102.07488 [hep-ph]].
- [76] G. J. Ding, S. F. King and C. Y. Yao, [arXiv:2103.16311 [hep-ph]].
- [77] H. Kuranaga, H. Ohki and S. Uemura, [arXiv:2105.06237 [hep-ph]].
- [78] T. Kobayashi and S. Tamba, Phys. Rev. D **99** (2019) no.4, 046001 [arXiv:1811.11384 [hep-th]].
- [79] A. Baur, H. P. Nilles, A. Trautner and P. K. S. Vaudrevange, Phys. Lett. B **795** (2019) 7 [arXiv:1901.03251 [hep-th]].
- [80] T. Kobayashi, Y. Shimizu, K. Takagi, M. Tanimoto and T. H. Tatsuishi, Phys. Rev. D **100** (2019) no.11, 115045, Erratum: [Phys. Rev. D **101** (2020) no.3, 039904] [arXiv:1909.05139 [hep-ph]].
- [81] H. P. Nilles, S. Ramos-Sánchez and P. K. S. Vaudrevange, JHEP **02** (2020), 045 [arXiv:2001.01736 [hep-ph]].
- [82] H. P. Nilles, S. Ramos-Sánchez and P. K. S. Vaudrevange, Nucl. Phys. B **957** (2020), 115098 [arXiv:2004.05200 [hep-ph]].
- [83] K. Ishiguro, T. Kobayashi and H. Otsuka, [arXiv:2010.10782 [hep-th]].
- [84] S. Kikuchi, T. Kobayashi, S. Takada, T. H. Tatsuishi and H. Uchida, Phys. Rev. D **102** (2020) no.10, 105010 [arXiv:2005.12642 [hep-th]].

- [85] S. Kikuchi, T. Kobayashi, H. Otsuka, S. Takada and H. Uchida, JHEP **11** (2020), 101 [arXiv:2007.06188 [hep-th]].
- [86] T. Kobayashi and H. Otsuka, Phys. Rev. D **102** (2020) no.2, 026004 [arXiv:2004.04518 [hep-th]].
- [87] G. J. Ding, F. Feruglio and X. G. Liu, JHEP **01** (2021), 037 [arXiv:2010.07952 [hep-th]].
- [88] K. Ishiguro, T. Kobayashi and H. Otsuka, JHEP **03** (2021), 161 [arXiv:2011.09154 [hep-ph]].
- [89] T. Kobayashi, Y. Shimizu, K. Takagi, M. Tanimoto, T. H. Tatsuishi and H. Uchida, Phys. Rev. D **101** (2020) no.5, 055046 [arXiv:1910.11553 [hep-ph]].
- [90] K. Hoshiya, S. Kikuchi, T. Kobayashi, Y. Ogawa and H. Uchida, PTEP **2021** (2021) no.3, 033B05 [arXiv:2012.00751 [hep-th]].
- [91] S. Kikuchi, T. Kobayashi and H. Uchida, [arXiv:2101.00826 [hep-th]].
- [92] G. J. Ding, F. Feruglio and X. G. Liu, SciPost Phys. **10** (2021), 133 [arXiv:2102.06716 [hep-ph]].
- [93] H. P. Nilles, S. Ramos-Sánchez and P. K. S. Vaudrevange, Phys. Lett. B **808** (2020), 135615 [arXiv:2006.03059 [hep-th]].
- [94] A. Baur, M. Kade, H. P. Nilles, S. Ramos-Sanchez and P. K. S. Vaudrevange, JHEP **02** (2021), 018 [arXiv:2008.07534 [hep-th]].
- [95] H. P. Nilles, S. Ramos-Sánchez and P. K. S. Vaudrevange, Nucl. Phys. B **966** (2021), 115367 [arXiv:2010.13798 [hep-th]].
- [96] A. Baur, M. Kade, H. P. Nilles, S. Ramos-Sanchez and P. K. S. Vaudrevange, Phys. Lett. B **816** (2021), 136176 [arXiv:2012.09586 [hep-th]].
- [97] A. Baur, M. Kade, H. P. Nilles, S. Ramos-Sánchez and P. K. S. Vaudrevange, [arXiv:2104.03981 [hep-th]].
- [98] P. Ko, T. Kobayashi, J. h. Park and S. Raby, Phys. Rev. D **76**, 035005 (2007) [erratum: Phys. Rev. D **76**, 059901 (2007)] [arXiv:0704.2807 [hep-ph]].
- [99] H. Ishimori, T. Kobayashi, H. Ohki, Y. Omura, R. Takahashi and M. Tanimoto, Phys. Rev. D **77**, 115005 (2008) [arXiv:0803.0796 [hep-ph]].
- [100] H. Ishimori, T. Kobayashi, Y. Omura and M. Tanimoto, JHEP **12**, 082 (2008) [arXiv:0807.4625 [hep-ph]].
- [101] H. Ishimori, T. Kobayashi, H. Okada, Y. Shimizu and M. Tanimoto, JHEP **12**, 054 (2009) [arXiv:0907.2006 [hep-ph]].
- [102] M. Dimou, S. F. King and C. Luhn, Phys. Rev. D **93**, no.7, 075026 (2016) doi:10.1103/PhysRevD.93.075026 [arXiv:1512.09063 [hep-ph]].
- [103] V. S. Kaplunovsky and J. Louis, Phys. Lett. B **306**, 269-275 (1993) [arXiv:hep-th/9303040 [hep-th]].

- [104] A. Brignole, L. E. Ibanez and C. Munoz, Nucl. Phys. B **422**, 125-171 (1994) [erratum: Nucl. Phys. B **436**, 747-748 (1995)] [arXiv:hep-ph/9308271 [hep-ph]].
- [105] T. Kobayashi, D. Suematsu, K. Yamada and Y. Yamagishi, Phys. Lett. B **348**, 402-410 (1995) [arXiv:hep-ph/9408322 [hep-ph]].
- [106] L. E. Ibanez, C. Munoz and S. Rigolin, Nucl. Phys. B **553**, 43-80 (1999) [arXiv:hep-ph/9812397 [hep-ph]].
- [107] P. P. Novichkov, J. T. Penedo, S. T. Petcov and A. V. Titov, JHEP **1907** (2019) 165 [arXiv:1905.11970 [hep-ph]].
- [108] G. Ecker, W. Grimus and W. Konetschny, Nucl. Phys. B **191** (1981), 465-492.
- [109] G. Ecker, W. Grimus and H. Neufeld, Nucl. Phys. B **247** (1984), 70-82.
- [110] G. Ecker, W. Grimus and H. Neufeld, J. Phys. A **20** (1987), L807.
- [111] H. Neufeld, W. Grimus and G. Ecker, Int. J. Mod. Phys. A **3** (1988), 603-616.
- [112] W. Grimus and M. N. Rebelo, Phys. Rept. **281** (1997), 239-308 [arXiv:hep-ph/9506272 [hep-ph]].
- [113] W. Grimus and L. Lavoura, Phys. Lett. B **579** (2004) 113. [hep-ph/0305309].
- [114] Z. Maki, M. Nakagawa and S. Sakata, Prog. Theor. Phys. **28** (1962) 870.
- [115] B. Pontecorvo, Sov. Phys. JETP **26** (1968) 984 [Zh. Eksp. Teor. Fiz. **53** (1967) 1717].
- [116] V. Andreev *et al.* [ACME], Nature **562** (2018) no.7727, 355-360.
- [117] D. M. Kara, I. J. Smallman, J. J. Hudson, B. E. Sauer, M. R. Tarbutt and E. A. Hinds, New J. Phys. **14** (2012), 103051 [arXiv:1208.4507 [physics.atom-ph]].
- [118] W. C. Griffith, Plenary talk at "Interplay between Particle & Astroparticle physics 2014", <https://indico.ph.qmul.ac.uk/indico/conferenceDisplay.py?confId=1>.
- [119] M. Fujiwara, J. Hisano, C. Kanai and T. Toma, JHEP **04** (2021), 114 [arXiv:2012.14585 [hep-ph]].
- [120] M. Fujiwara, J. Hisano and T. Toma, [arXiv:2106.03384 [hep-ph]].
- [121] E. Ma and G. Rajasekaran, Phys. Rev. D **64**, 113012 (2001) [arXiv:hep-ph/0106291].
- [122] K. S. Babu, E. Ma and J. W. F. Valle, Phys. Lett. B **552**, 207 (2003) [arXiv:hep-ph/0206292].
- [123] G. Altarelli and F. Feruglio, Nucl. Phys. B **720** (2005) 64 [hep-ph/0504165].
- [124] G. Altarelli and F. Feruglio, Nucl. Phys. B **741** (2006) 215 [hep-ph/0512103].
- [125] Y. Shimizu, M. Tanimoto and A. Watanabe, Prog. Theor. Phys. **126** (2011) 81 [arXiv:1105.2929 [hep-ph]].

- [126] S. T. Petcov and A. V. Titov, Phys. Rev. D **97** (2018) no.11, 115045 [arXiv:1804.00182 [hep-ph]].
- [127] S. K. Kang, Y. Shimizu, K. Takagi, S. Takahashi and M. Tanimoto, PTEP **2018**, no. 8, 083B01 (2018) [arXiv:1804.10468 [hep-ph]].
- [128] H. Okada, Y. Shimizu, M. Tanimoto and T. Yoshida, [arXiv:2105.14292 [hep-ph]].
- [129] A. M. Baldini *et al.* [MEG], Eur. Phys. J. C **76** (2016) no.8, 434 doi:10.1140/epjc/s10052-016-4271-x [arXiv:1605.05081 [hep-ex]].
- [130] F. Feruglio, C. Hagedorn, Y. Lin and L. Merlo, Nucl. Phys. B **832**, 251-288 (2010) [arXiv:0911.3874 [hep-ph]].
- [131] H. Ishimori and M. Tanimoto, Prog. Theor. Phys. **125** (2011), 653-675 [arXiv:1012.2232 [hep-ph]].
- [132] G. C. Branco, R. G. Felipe and F. R. Joaquim, Rev. Mod. Phys. **84** (2012) 515 [arXiv:1111.5332 [hep-ph]].
- [133] M. Holthausen, M. Lindner and M. A. Schmidt, JHEP **1304** (2013) 122 [arXiv:1211.6953 [hep-ph]].
- [134] M. C. Chen, M. Fallbacher, K. T. Mahanthappa, M. Ratz and A. Trautner, Nucl. Phys. B **883** (2014) 267 [arXiv:1402.0507 [hep-ph]].
- [135] F. Feruglio, C. Hagedorn and R. Ziegler, JHEP **07** (2013), 027 [arXiv:1211.5560 [hep-ph]].
- [136] S. Ferrara, D. Lust, A. D. Shapere and S. Theisen, Phys. Lett. B **225**, 363 (1989).
- [137] M. Chen, S. Ramos-Sánchez and M. Ratz, Phys. Lett. B **801** (2020), 135153 [arXiv:1909.06910 [hep-ph]].
- [138] R. C. Gunning, *Lectures on Modular Forms* (Princeton University Press, Princeton, NJ, 1962).
- [139] B. Schoeneberg, *Elliptic Modular Functions* (Springer-Verlag, 1974).
- [140] N. Koblitz, *Introduction to Elliptic Curves and Modular Forms* (Springer-Verlag, 1984).
- [141] S. P. Martin and M. T. Vaughn, Phys. Rev. D **50**, 2282 (1994) [Erratum-ibid. D **78**, 039903 (2008)] [arXiv:hep-ph/9311340].
- [142] S. P. Martin, Adv. Ser. Direct. High Energy Phys. **18** (1998), 1-98 [arXiv:hep-ph/9709356 [hep-ph]].
- [143] J. Hisano, M. Nagai and P. Paradisi, Phys. Rev. D **78**, 075019 (2008) [arXiv:0712.1285 [hep-ph]].
- [144] F. Borzumati and A. Masiero, Phys. Rev. Lett. **57**, 961 (1986).
- [145] F. Gabbiani, E. Gabrielli, A. Masiero and L. Silvestrini, Nucl. Phys. B **477**, 321 (1996) [arXiv:hep-ph/9604387].

- [146] W. Altmannshofer, A. J. Buras, S. Gori, P. Paradisi and D. M. Straub, Nucl. Phys. B **830** (2010), 17-94 [arXiv:0909.1333 [hep-ph]].
- [147] U. Sarkar [CMS], [arXiv:2105.01629 [hep-ex]].
- [148] A. Kalogeropoulos [ATLAS and CMS], PoS LHCP2020 (2021), 166.
- [149] I. Esteban, M. C. Gonzalez-Garcia, M. Maltoni, T. Schwetz and A. Zhou, JHEP **09** (2020), 178 [arXiv:2007.14792 [hep-ph]].
- [150] S. Antusch and V. Maurer, JHEP **1311** (2013) 115 [arXiv:1306.6879 [hep-ph]].
- [151] F. Björkeröth, F. J. de Anda, I. de Medeiros Varzielas and S. F. King, JHEP **1506** (2015) 141 [arXiv:1503.03306 [hep-ph]].
- [152] A. M. Baldini *et al.* [MEG II], Eur. Phys. J. C **78** (2018) no.5, 380 [arXiv:1801.04688 [physics.ins-det]].
- [153] A. Blondel, A. Bravar, M. Pohl, S. Bachmann, N. Berger, M. Kiehn, A. Schoning, D. Wiedner, B. Windelband and P. Eckert, *et al.* [arXiv:1301.6113 [physics.ins-det]].
- [154] R. J. Abrams *et al.* [Mu2e], [arXiv:1211.7019 [physics.ins-det]].
- [155] R. Abramishvili *et al.* [COMET], PTEP 2020 (2020) no.3, 033C01 [arXiv:1812.09018 [physics.ins-det]].
- [156] J. h. Park, Phys. Rev. D **83** (2011), 055015 doi:10.1103/PhysRevD.83.055015 [arXiv:1011.4939 [hep-ph]].
- [157] P. A. Zyla *et al.* [Particle Data Group], PTEP 2020 (2020) no.8, 083C01.
- [158] J. Hisano, T. Moroi, K. Tobe, M. Yamaguchi and T. Yanagida, Phys. Lett. B **357**, 579 (1995) [arXiv:hep-ph/9501407].
- [159] J. Hisano, T. Moroi, K. Tobe and M. Yamaguchi, Phys. Rev. D **53**, 2442 (1996) [arXiv:hep-ph/9510309].